geologica acta

Citation: Bover-Arnal, T., Strasser, A., Salas, R., 2024.Fossil corals with skeletal lesions comparable to modern ones. Geologica Acta, 22.9, 1-23.
Online ISSN: 1696-5728 DOI: 10.1344/GeologicaActa2024.22.9

Fossil corals with skeletal lesions comparable to modern ones

Telm Bover-Arnal[1,2] **André Strasser**[3] **Ramon Salas**[1,2]

[1]**Departament de Mineralogia, Petrologia i Geologia Aplicada, Facultat de Ciències de la Terra, Universitat de Barcelona**
c/Martí i Franquès s/n, 08028 Barcelona, Catalonia, Spain.
Bover-Arnal E-mail: telm.boverarnal@ub.edu Salas E-mail: ramonsalas@ub.edu

[2]**Institut de Recerca GEOMODELS**
c/ Martí i Franquès s/n, 08028 Barcelona, Catalonia, Spain.

[3]**Département de Géosciences, Université de Fribourg**
Chemin du Musée 6, 1700 Fribourg, Switzerland.
Strasser E-mail: andreas.strasser@unifr.ch

ABSTRACT

Whereas post-mortem bioerosional features such as bivalve, sponge or worm borings are frequently preserved in ancient corals, reports of ante-mortem skeletal anomalies on Cretaceous specimens are rare. Here, we document the occurrence of fossil skeletal lesions produced during the life span of the colonies in exceptionally well-preserved Aptian (Early Cretaceous) scleractinians from the Maestrat Basin (East Iberia). These ante-mortem damage features are characterized by millimetric to centimetric areas of skeletal depression, as well as upward growth around damaged areas indicating regeneration. Depressed skeletal lesions are commonly overprinted by post-mortem lithophagid borings. Distribution of skeletal anomalies on the colonies can be focal or multifocal, and their location basal, medial and/or apical. The extent of the skeletal anomalies can be mild (occupying <10% of the colony) to extreme (occupying ≥50% of the colony). The edges of the skeletal anomalies are distinct (disk-shaped) or annular (ring-shaped), the margins are mainly smooth to uneven, and the shapes are circular, oblong, pyriform, linear, or irregular. The skeletal anomalies exhibited by the corals are comparable to tissue lesions produced in modern corals either by predation, bioerosion or disease, which may be followed by skeletal overgrowth or denudation. Although demonstrating disease in fossil colonies is challenging, there is no reason to believe that corals did not experience diseases back in the Cretaceous. This paper gives an example of the potential of coral anomalies originating from tissue lesions and skeletal damage to be preserved in the geological record, a factor that may have been often overlooked in the study of fossil coral communities.

KEYWORDS **Coral. Skeletal anomaly. Lesion. Iberian Chain. Aptian.**

INTRODUCTION

Current global warming is having detrimental effects on tropical to subtropical shallow-water scleractinian colonies (*e.g.* Hoegh-Guldberg *et al.*, 2017; van der Zande *et al.*, 2020). The increase in shallow seawater temperatures is exacerbating coral disease outbreaks (*e.g.* Maynard *et al.*, 2015) and producing increased frequency and severity of storms (*e.g.* Knutson *et al.*, 2010). Storms adversely affect coral populations through sediment overloading and physical impacts. Additional stressors on corals include tissue predation and skeleton damage caused by corallivores, such as certain species of fish, annelids, crustaceans, echinoderms, and molluscs (see Rotjan and

Lewis, 2008). Furthermore, ocean acidification slows down the growth and regeneration potential of the coral skeletons (*e.g.* Hoegh-Guldberg *et al.*, 2017; van der Zande *et al.*, 2020).

The effects of sediment overloading on modern corals, damage caused by storms, predation, bioerosion and disease are widespread, visible, and tangible (*e.g.* Morais *et al.*, 2022a, b; Sutherland *et al.*, 2004). Therefore, concern on the health of low-latitude coral ecosystems of the planet has taken a deep root in academia, media, and society. These disturbing impacts provoke tissue loss lesions on corals and subsequent denuded skeleton scars, which commonly exhibit clearly defined margins between the denuded skeleton and the coral's living tissue (*e.g.* Aeby *et al.*, 2019). Disease can also result in irregular skeletal deposition, *i.e.* growth anomalies (*e.g.* Work *et al.*, 2008). Dead and depressed parts of coral skeletons are usually rapidly colonized by encrusting red algae, soft green and brown algae, and microbial films. Endolithic organisms such as cyanobacteria, algae, sponges, worms and bivalves perforate the dead skeleton (*e.g.* Medellín-Maldonado *et al.*, 2023). The activity of endoliths also results in discrete features of skeleton loss (*e.g.* Scoffin and Bradshaw, 2000).

Whereas post-mortem bioerosion features produced by infaunal sponges, worms and bivalves are commonly observable on Phanerozoic fossil corals (*e.g.* Tapanila and Copper, 2002; Vogel, 1993), reports of ante-mortem physical signatures indicating similar stresses on Mesozoic coral populations are rare, perhaps limited to those of endolithic microbioerosion on Oxfordian–Kimmeridgian, Barremian–Aptian and Cenomanian colonial corals (Kołodziej *et al.*, 2012, 2016; Salamon *et al.*, 2021, 2022). Sanders and Baron-Szabo (2005) also reported growth anomalies in Upper Cretaceous corals from the Pyrenees and Austria, interpreted as resulting from colony toppling and sediment accumulation. On the other hand, Cenozoic examples of skeletal anomalies generated during the life of the coral are more abundant: they have been interpreted as being related to predation and sediment overloading (*e.g.* Álvarez-Pérez and Busquets, 2012), as well as to symbiotic associations with barnacles and other organisms such as molluscs, crabs, brachiopods, sipunculans and polychaetes (see *e.g.* Klompmaker *et al.*, 2016; Santos *et al.*, 2012, and references therein). Embedment of organisms inside the growing skeletons of corals have been widely reported also from Ordovician to Devonian communities (*e.g.* Elias, 1986; Falces, 1997; Oliver, 1983; Tapanila, 2005, 2006; Tapanila and Holmer, 2006; Tapanila and Ekdale, 2007). Skeletal damage and subsequent repair on rugose corals have been documented from Ordovician and Carboniferous populations (Elias, 1984; Webb and Yancey, 2010).

This paper reports on remarkable ante-mortem macro-skeletal anomalies, as well as post-mortem bioerosion structures, identified in Aptian (Early Cretaceous) coral populations from the Maestrat Basin (Eastern Iberian Chain). Ante-mortem coral skeletal damage observed in the fossil specimens is compared to lesions in modern corals. This comparative analysis aims to gain understanding of how Aptian scleractinians thriving in carbonate platform environments interacted with their surrounding environment, and how they were affected by marine processes and the coexisting biological community.

GEOLOGICAL SETTING

The fossil scleractinians studied occur in the Maestrat Basin, which is located in the eastern part of the Iberian Plate (Fig. 1A). The Maestrat Basin was formed by two rifting cycles of Kimmeridgian-early Berriasian and Barremian-early Albian ages (Salas *et al.* in Martín-Chivelet *et al.*, 2019) that resulted from the opening of the North Atlantic and the Bay of Biscay, respectively (Salas and Casas, 1993; Salas *et al.*, 2001, 2010). Throughout the Late Jurassic-Early Cretaceous, a thick (>1.5km) continental to marine mixed carbonate-siliciclastic sedimentary succession accumulated in depocentral areas of the basin (*e.g.* Salas, 1987). The Mesozoic sedimentary record was inverted during the late Eocene-early Miocene on account of the Alpine orogeny and now forms the Iberian Chain (Fig. 1A; *e.g.* Guimerà, 1994, 2018).

The colonial corals analysed are found in the Galve Sub-basin, which corresponds to the western depocentre of the Maestrat Basin (Salas *et al.* in Martín-Chivelet *et al.*, 2019). During the Late Jurassic-Early Cretaceous extension, this sub-basin was separated from neighbouring depocentres by major normal faults (Salas *et al.* in Martín-Chivelet *et al.*, 2019). The present structure of the Galve Sub-basin resulted from the Alpine contraction and consists of two main folds: the Miravete anticline and the Camarillas syncline (Liesa *et al.*, 2006; Simón, 2004; Fig. 1B).

The Aptian sedimentary succession containing the scleractinians studied crops out along the limbs of these two folds (Fig. 1B). This rock record can be subdivided into three marine lithostratigraphic units with the rank of formations (*e.g.* Bover-Arnal *et al.*, 2016). The oldest Aptian unit, the Forcall Formation, corresponds to basinal marls and limestones with *Palorbitolina lenticularis* and ammonoids. This unit overlies the Xert Formation which consists of upper Barremian coastal sandstones and sandy limestones, and platform carbonates with *Palorbitolina lenticularis* and *Chondrodonta* (*e.g.* Bover-Arnal *et al.*, 2016; Fig. 1C). The lowermost part of the Forcall

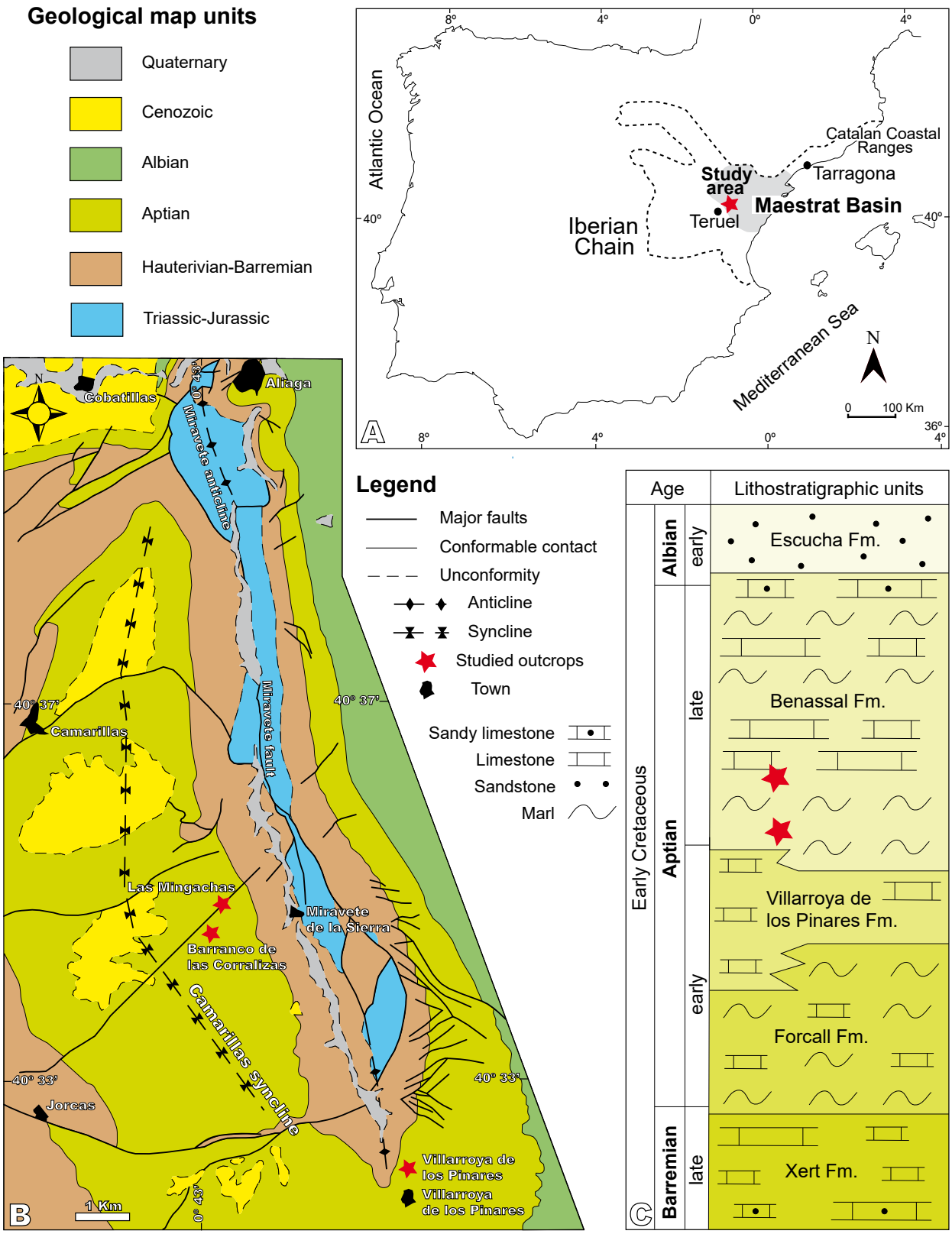

FIGURE 1. Geological setting. A) Geographical location of the study area in the western Maestrat Basin (Eastern Iberian Chain). B) Geological map of the Galve Sub-basin. The outcrops studied are indicated with red stars. Modified after Canérot *et al.* (1979) and Gautier (1980). C) Chrono- and lithostratigraphy of the Galve Sub-basin after Bover-Arnal *et al.* (2016). The stratigraphic levels bearing the coral colonies analysed are indicated with red stars.

Formation is latest Barremian in age, whereas the rest of the formation recorded the four early Aptian ammonoid zones: *Deshayesites oglanlensis*, *Deshayesites forbesi*, *Deshayesites deshayesi* and *Dufrenoyia furcata* (Moreno-Bedmar *et al.*, 2010; Garcia *et al.*, 2014). In the Galve Sub-basin, the Forcall Formation also encompasses a limestone horizon characterized by a distinctive facies of *Lithocodium aggregatum* and corals (Bover-Arnal *et al.*, 2011; Vennin and Aurell, 2001). These *Lithocodium*-bearing beds are located in the upper part of the *Deshayesites forbesi* biozone and were contemporaneous with segment C4 of the early Aptian oceanic anoxic event 1a (Cors *et al.*, 2015).

Overlying the Forcall Formation there is the upper lower Aptian Villarroya de los Pinares Formation (Fig. 1C), which is made up of platform carbonates characterized by the presence of rudist bivalves and corals (*e.g.* Bover-Arnal *et al.*, 2010; Gili *et al.*, 2016). Above, the uppermost lower-upper Aptian Benassal Formation (Fig. 1C) is mainly constituted by an alternation between distal marly intervals with colonial corals and *Trochonerita gigas*, and platform top carbonates with corals, rudists, and nerineid gastropods (*e.g.* Bover-Arnal *et al.*, 2016). In the Galve Sub-basin, the Benassal Formation displays two or three transgressive-regressive cycles, depending on the specific area (Bover-Arnal *et al.*, 2016). Each cycle consists of a lower transgressive marly interval followed by an upper regressive platform top limestone interval (Fig. 1C). The upper regressive part of the third cycle of the Benassal Formation, however, recorded an evolution towards more proximal, coastal depositional environments where grainstones with ferruginous ooids, sandy limestones and sandstones deposited (Bover-Arnal *et al.*, 2016). The marly base of the Benassal Formation contains *Dufrenoyia dufrenoyi* ammonite specimens, which indicate a latest early Aptian age (Bover-Arnal *et al.*, 2014; Moreno-Bedmar *et al.*, 2012). Above, the late Aptian ammonoid zones *Epicheloniceras martini*, *Parahoplites melchioris* and *Acanthohoplites nolani* have been respectively recognised in the lower, middle, and upper marly parts of the Benassal Formation (Bover-Arnal *et al.*, 2016). The original, and more exhaustive, descriptions of these Aptian lithostratigraphic units can be found in Canérot *et al.* (1982) and Salas (1987).

The Aptian scleractinians exhibiting skeletal anomalies analysed herein occur at the base and the top of the first marly interval of the Benassal Formation (Fig. 1C), and thus are latest early-early late Aptian in age (*Dufrenoyia furcata* and *Epicheloniceras martini* ammonite zones). Aptian corals in the Galve Sub-basin are also present in the marls and limestones of the Forcall Formation (Bover-Arnal *et al.*, 2011; Vennin and Aurell, 2001) and in the rudist-bearing limestones of the Villarroya de los Pinares and Benassal formations (Bover-Arnal *et al.*, 2015).

Taxonomy and palaeoecology of the Aptian corals from the Galve Sub-basin

Bover-Arnal *et al.* (2012) studied the taxonomy and palaeoecology of scleractinians occurring in Aptian rocks of the Galve Sub-basin. The coral fauna identified included mainly common Early Cretaceous genera and species of the families Archeocaeniidae, Faviidae, Fungiidae, and Microsolenidae such as *Stelidioseris actinastrae*, *Actinastraeopsis catalaunica*, *Placocolumastrea affinis*, *Diplogyra* cf. *minima*, *Diplogyra* sp., *Eohydnophora tenuis*, *Eohydnophora picteti*, *Eohydnophora tosaensis*, *Complexastrea* sp., *Camptodocis* cf. *tottoni*, *Camptodocis* sp., *Holocoenia bendukidzeae*, *Mesomorpha* cf. *mammillata*, *Ovalastrea* sp., *Thalamocaeniopsis* sp., *Thalamocaeniopsis ouenzensis*, *Eocomoseris raueni*, *Polyphylloseris* cf. *kobyi* and *Polyphylloseris simondsi*. However, rare genera in the Early Cretaceous record such as *Agrostyliastraea* sp. and *Procladocora* sp. also occur.

The coral colonies examined by Bover-Arnal *et al.* (2012) are autochthonous and show a predominance of decimetre-sized flattened-massive (Fig. 2A), branching (Fig. 2B) and domal (Fig. 2C-F) forms. Most of these coral colonies settled sparsely, giving rise to a continuous and uniform unbound growth fabric (Fig. 3; see Insalaco, 1998). Nevertheless, locally, the scleractinians occur fused into small metre-sized banks (Bover-Arnal *et al.*, 2012). These non-reef-building level-bottom communities flourished on slope settings, as coral meadows or coral carpets on marly or platform top-derived carbonate substrates (Figs. 2-3) under calm hydrodynamic conditions. The corals occurring embedded in marls (Fig. 2D-E) commonly show bioerosional structures indicating exposure to endolithic organisms after the death of the colony, thus implying low sedimentation rates. On the other hand, the colonies overlain by carbonate shed from the platform top (Fig. 2F) are usually devoid of bioerosional structures, indicating rapid burial of a living coral (Bover-Arnal *et al.*, 2012).

MATERIALS AND METHODS

In the Galve Sub-basin (Fig. 1B), Aptian scleractinians are found in growth position in both platform top carbonates and marly platform slopes (*e.g.* Bover-Arnal *et al.*, 2009, 2010). The corals occurring in uniformly weathered platform top limestones appear as a section, displaying only two dimensions (see *e.g.* Bover-Arnal *et al.*, 2009, 2015). Consequently, analysing the entire colony is not feasible in such cases. On the contrary, colonial corals found in marls and marly limestones within slope depositional

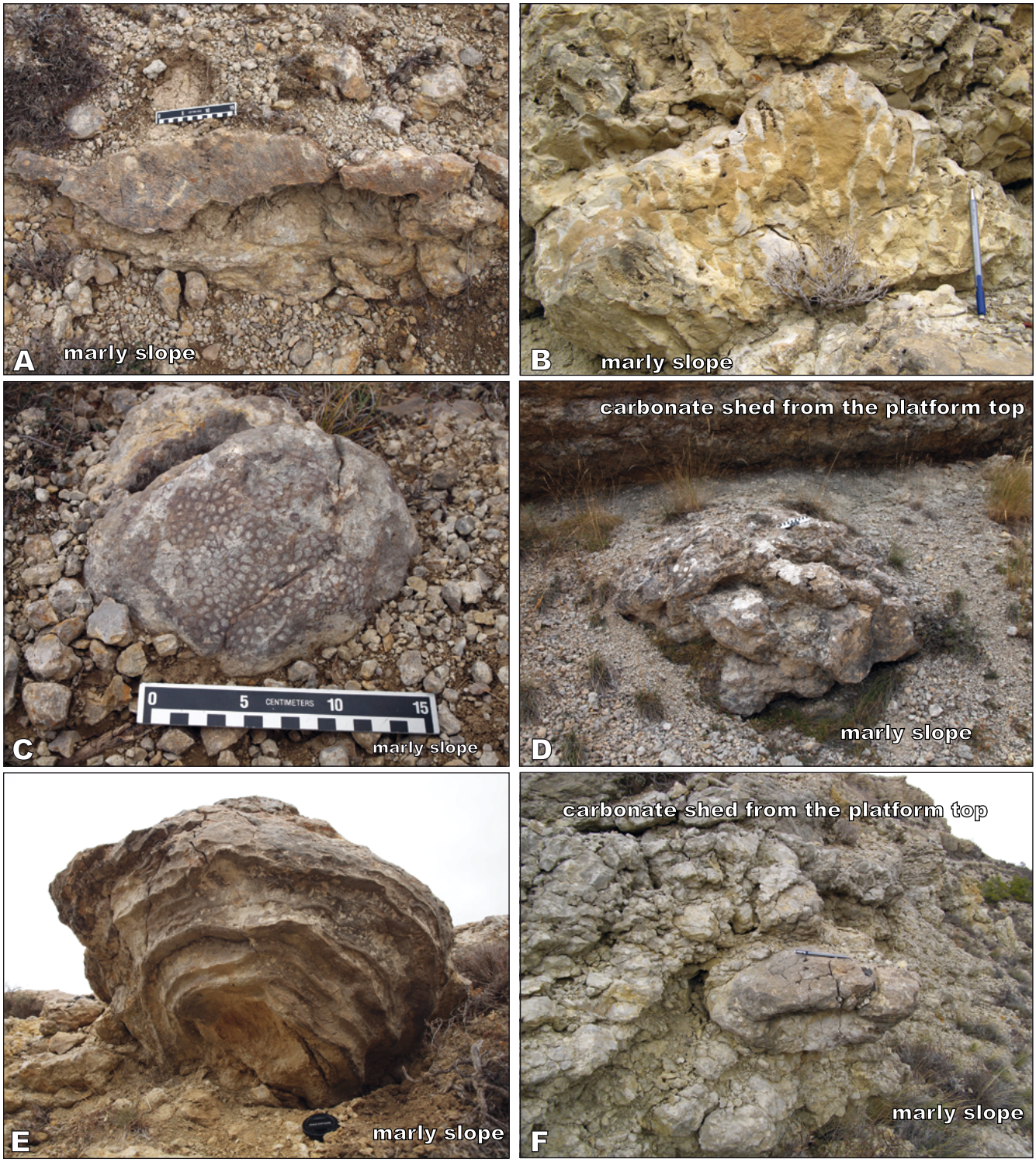

FIGURE 2. Close-up views of autochthonous Aptian scleractinian colonies from the marl-dominated slope environments of the lower part of the Benassal Formation. A) Flattened-massive colony from Villarroya de los Pinares. Ruler= 15cm. B) Branching coral from the Barranco de las Corralizas locality. Pencil= 14cm. C) Decimeter-sized isolated domal coral embedded in slope marls in Villarroya de los Pinares. D) Meter-sized isolated domal colony embedded in slope marls in the Barranco de las Corralizas. Ruler= 15cm. E) View of the underside of a colony that grew in marly slope environments in Villarroya de los Pinares, building superimposed dome-shaped structures. This growth pattern is also characteristic of present-day corals, such as the species *Montastrea cavernosa*. Camera cap= 5.8cm. F) An isolated domal colony overlain by carbonate shed from the platform top in the Barranco de las Corralizas. A pencil, measuring 14cm in length, is positioned above the scleractinian colony.

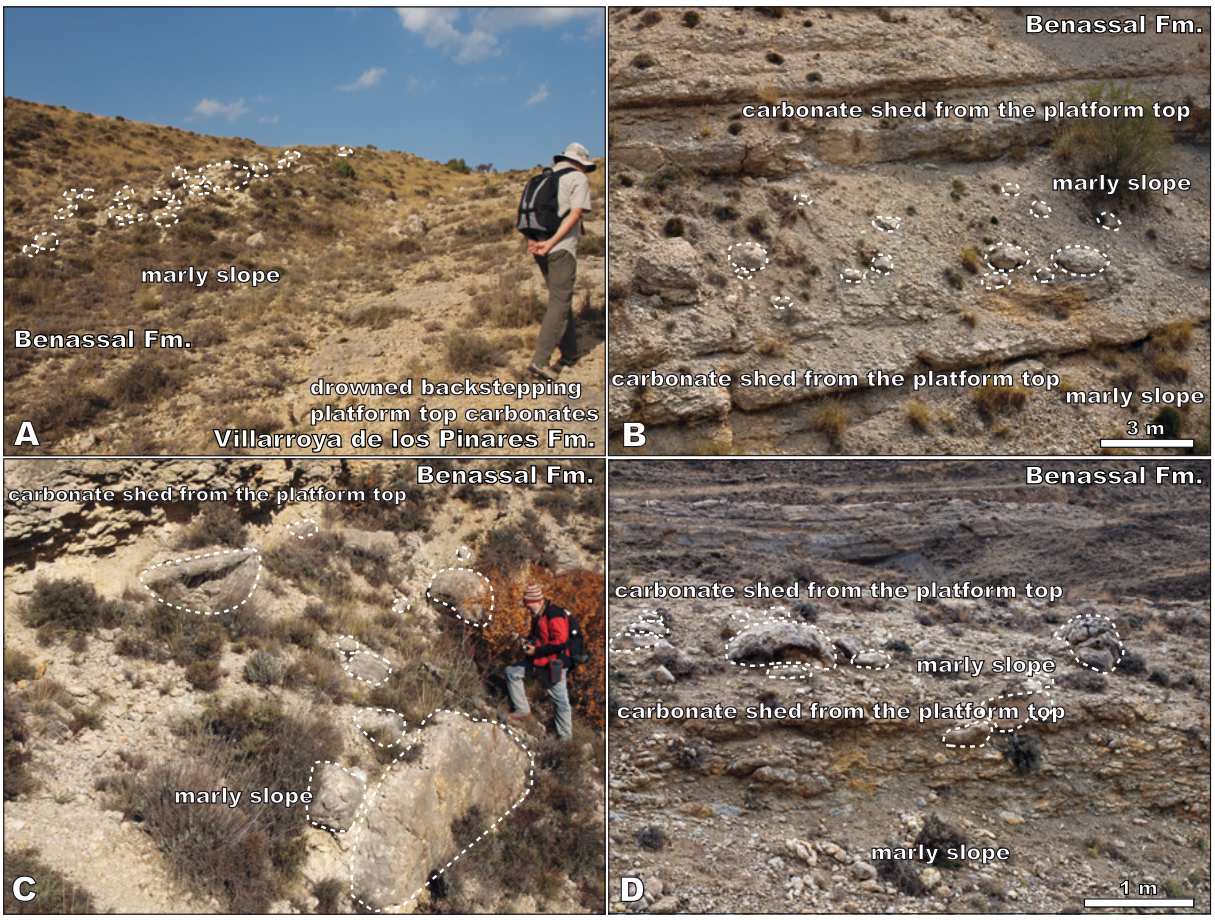

FIGURE 3. Outcrop-scale photographs of the marly intervals containing the autochthonous scleractinians investigated: A) Lower coral-bearing stratigraphic interval of Las Mingachas, B) and C) Barranco de las Corralizas, and D) Villarroya de los Pinares. The coral colonies are delineated by dashed white lines. Note the relatively high-density population and the laterally continuous but loose arrangement of the corals. When a bar scale is not available, use Ramon Salas as a reference for scale. See Figures 1B and 4 for geographical, geological and stratigraphical location of the outcrops.

environments are well-preserved and showcased in three dimensions, enabling a comprehensive examination of the whole colony (Figs. 2-3). Therefore, this study focuses on the latter corals.

The coral colonies whose skeletal anomalies were investigated occur in the marls of the lower part of the Benassal Formation, in three different localities (Fig. 1C): Las Mingachas (Fig. 4A), Barranco de las Corralizas (Fig. 4B) and Villarroya de los Pinares (Fig. 4C). In Las Mingachas (Fig. 1C), two stratigraphic intervals rich in corals were respectively surveyed at the lowermost (Fig. 3A) and uppermost parts of the lower marls of the Benassal Formation (Fig. 4A). A total of 102 scleractinian colonies were examined: 14 at the base of the Benassal Formation in Las Mingachas (Figs. 3A; 4A), 11 in the uppermost part of the lower marls of the Benassal Formation in Las Mingachas (Fig. 4A), 22 in the Barranco de las Corralizas (Figs. 3B-C; 4B) and 55 in Villarroya de los Pinares (Figs. 3D; 4C).

The workflow employed in this study began with documenting the colony growth form (flattened, massive, domal, branching), and measuring the diameter and height of each specimen analysed. The description of the skeletal anomalies exhibited by the corals is based on Work and Aeby (2006). These authors provide a framework focused on describing the morphology of gross lesions, defined as any change in tissues in living corals, which is therefore partly applicable to fossil coral anomalies. The descriptive features of skeletal anomalies documented in this paper are summarized in Figure 5 and Table 1. They include: i) skeletal anomaly relief (depressed, coniform), ii) skeletal anomaly shape (circular, oblong, pyriform, linear, irregular), iii) skeletal anomaly margin (smooth, uneven), iv) skeletal anomaly edge (distinct, annular), v) distribution of skeletal anomalies on colony (focal, multifocal), vi) location of skeletal anomalies on colony (basal, medial, apical) and vii) skeletal anomaly severity (mild <10%, moderate 10-24%, severe 25-49%, extreme ≥50%).

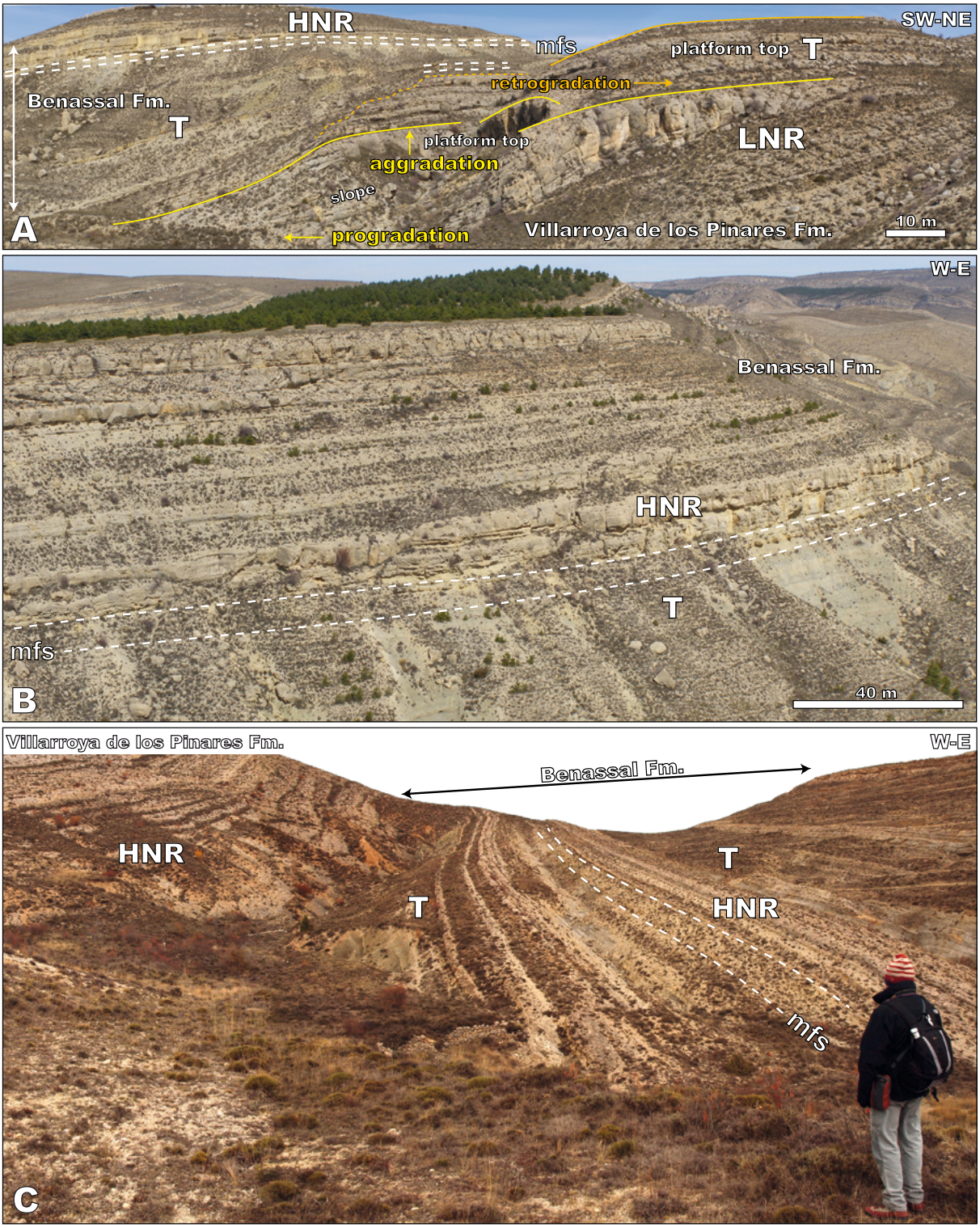

FIGURE 4. Panoramic photographs of A) Las Mingachas, B) Barranco de las Corralizas and C) Villarroya de los Pinares outcrops investigated. The stratigraphic levels bearing the coral colonies analysed are delimited between dashed white lines. HNR= Highstand Normal Regressive, T= Transgressive, LNR= Lowstand Normal Regressive, mfs= maximum flooding surface. In C) use Ramon Salas for scale. Note that the lower stratigraphic interval containing colonial corals examined in Las Mingachas was deposited during a transgressive stage of relative sea level and corresponds to marly slope environments retrograding above backstepping platform top carbonates. The other stratigraphic intervals investigated are located in the uppermost marly interval of the lower part of the Benassal Formation in Las Mingachas, Barranco de las Corralizas and Villarroya de los Pinares. This coral-bearing horizon overlies a maximum-flooding surface and, therefore, formed at the beginning of progradation over basinal marls of distal slope environments during early highstand normal regression. The sequence-stratigraphic interpretation is after Bover-Arnal *et al.* (2009, 2010, 2016). See Figure 1B for geographical and geological location of the outcrops.

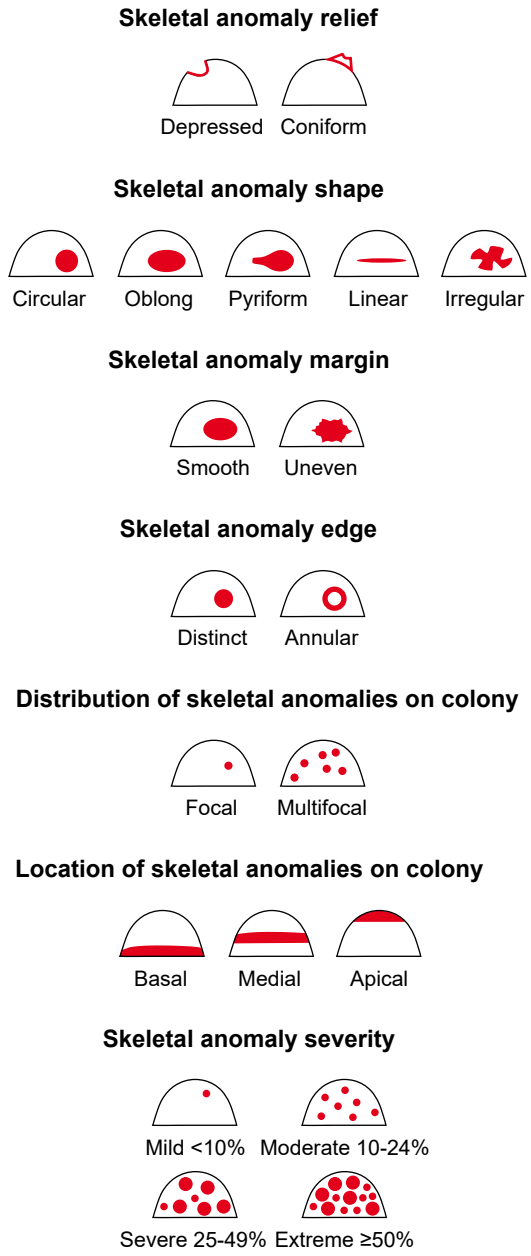

FIGURE 5. Categories (in bold type) and terms (normal text) used to describe the anomalies in the skeleton of fossil scleractinian corals (based on Work and Aeby, 2006).

The description of the fossil skeletal anomalies is illustrated with close-up views (Figs. 6-14). In addition, the anomalies are here compared with images of tissue lesions and damage captured on living and recent scleractinians (Figs. 6-12). The latter photographs were taken in 2011 and 2012 in various tropical reefs across Australia, specifically in the Houtman Abrolhos Islands and Ningaloo Reef in Western Australia, as well as in the Whitsundays, Lady Elliot, Heron, Wistari, and Knuckle reefs in Eastern Australia.

Vertical thin sections were prepared across the skeletal anomalies to determine whether corallites displayed modified growth or growth anomalies that could indicate responses to damage by the living coral (*e.g.* Work and Rameyer, 2005; Work and Aeby, 2010). However, the scleractinian skeletons, initially composed of aragonite, underwent diagenetic replacement to calcite and recrystallization during burial, resulting in the loss of the original internal growth microstructures. Consequently, the thin-section analyses were not conclusive.

To determine genus and species of the depicted fossils (Figs. 6-14) would entail disrupting colonies, sampling, and subsequent production of thin sections. This methodology was previously employed in Bover-Arnal *et al.* (2012), where poorly preserved and fragmented colonies were collected to preserve this exceptional fossil record. Thus, the absence of specific genera and species in the illustrated colonies is addressed by summarizing the taxonomic findings from 2012 (see previous section on taxonomy and palaeoecology) to preserve its integrity.

RESULTS

The smallest scleractinian colony analysed is 5cm in diameter and 3cm in height, whilst the largest colony is 230cm in diameter and 120cm in height (Fig. 3C). The mean diameter of the colonies is 40cm and the mean height 22cm. Out of 102 colonies, 72 exhibited skeletal anomalies (70.6%), 40 in Villarroya de los Pinares (Figs. 1B; 4C), 10 in the lowermost part of the Benassal Formation in Las Mingachas (Figs. 1B; 3A; 4A), 7 in the upper part of the lower marl unit of the Benassal Formation (Figs. 1B; 4A), and 15 in the Barranco de Las Corralizas (Figs. 1B; 4B). Most of the coral colonies exhibiting skeletal anomalies, 47 out of 72, exhibit more than one skeletal anomaly, and thus these colonies may present more than one term for certain categories such as skeletal anomaly relief, shape, margin, edge, and location (Table 1).

The skeletal anomalies investigated correspond to depressed areas of coral skeleton (Figs. 6-9; 11A; 12A; 14), or rare upward grown coniform structures (Fig. 10). The 94.6% of the colonies surveyed exhibiting damage structures display only depressed skeletal anomalies, occasionally accompanied by rare coniform overgrowth structures (2.7%) (Table 1). The shapes of the damage structures are mainly circular (Fig. 6A, C, E), oblong (Fig. 7A, C, E) and irregular (Figs. 9C, E; 11A; 12A), however pyriform (Fig. 8A) and linear (Fig. 8C, E) depressions are also common. Most of the colonies investigated show only irregular (44.4%), oblong and irregular (16.7%), or circular, oblong, and irregular (8.3%) anomalies (Table 1).

TABLE 1. Summarized results for each category and term used to describe fossil skeletal anomalies, presented in both absolute colony values (n) and percentages (%). Bear in mind that 47 out of the 72 coral colonies with damage features exhibit more than one skeletal anomaly, and that these colonies may present more than one term for certain categories

Total of colonies surveyed			
n=102 (**100%**)			
Not exhibiting skeletal anomalies	**Exhibiting skeletal anomalies**		
n=30 (**29.4%**)	n=72 (**70.6%**)		
	Category	**Term**	
	Skeletal anomaly relief	Coniform	n=2 (**2.7%**)
		Depressed	n=68 (**94.6%**)
		Depressed; Coniform	n=2 (**2.7%**)
	Skeletal anomaly shape	Circular	n=2 (**2.8%**)
		Oblong	n=2 (**2.8%**)
		Linear	n=1 (**1.4%**)
		Irregular	n=32 (**44.4%**)
		Circular; Linear	n=1 (**1.4%**)
		Circular; Irregular	n=4 (**5.5%**)
		Oblong; Irregular	n=12 (**16.7%**)
		Pyriform; Irregular	n=2 (**2.8%**)
		Linear; Irregular	n=2 (**2.8%**)
		Circular; Oblong; Irregular	n=6 (**8.3%**)
		Circular; Linear; Irregular	n=4 (**5.5%**)
		Circular; Pyriform; Irregular	n=1 (**1.4%**)
		Oblong; Pyriform; Irregular	n=1 (**1.4%**)
		Circular; Oblong; Linear; Irregular	n=2 (**2.8%**)
	Skeletal anomaly margin	Smooth	n=49 (**68%**)
		Uneven	n=8 (**11.1%**)
		Smooth; Uneven	n=15 (**20.9%**)
	Skeletal anomaly edge	Distinct	n=68 (**94.4%**)
		Annular	n=1 (**1.4%**)
		Distinct; Annular	n=3 (**4.2%**)
	Distribution of skeletal anomalies on colony	Focal	n=25 (**34.8%**)
		Multifocal	n=47 (**65.2%**)
	Location of skeletal anomalies on colony	Medial	n=5 (**7%**)
		Apical	n=40 (**55.5%**)
		Basal; Medial	n=1 (**1.4%**)
		Medial; Apical	n=22 (**30.6%**)
		Basal; Medial; Apical	n=4 (**5.5%**)
	Skeletal anomaly severity	Mild (<10%)	n=27 (**37.5%**)
		Moderate (10-24%)	n=27 (**37.5%**)
		Severe (25-49%)	n=17 (**23.6%**)
		Extreme (50-100%)	n=1 (**1.4%**)

n=sample size

The depressed circular skeletal anomalies (Fig. 6A, C, E) display diameters of 0.8 to 13.5cm and depths between 0.5 and 7cm, with a mean diameter of 6.9cm and a mean depth of 2.6cm. Locally, circular depressions show overgrown margins (*e.g.* Fig. 6A). The depressed oblong skeletal anomalies (Fig. 7A, C, E) exhibit lengths between 2.2 and 36cm, widths between 1 and 5cm, and depths between 1 and 19cm, with means of 9.9, 2.5, and 3.6cm, respectively. The skeletal anomalies with irregular shapes and depressed reliefs (Figs. 9C, E; 11A; 12A) range in length from 2.5 to 44cm, widths from 1 to 15cm, and depths from 1 to 14cm, with respective means of 16cm, 6.2cm, and 4.8cm. Pyriform depressions (Fig. 8A) have lengths between 9 and 19cm, with a mean of 13.4cm, widths around 2cm, and depths ranging from 2 to 6cm, with a mean of 4.4cm. Skeletal anomalies with linear depressions (Fig. 8C, E) exhibit lengths ranging from 5 to 10cm, with a mean of 2cm, widths ranging from 0.2 to 6cm, with a mean of 3.9cm, and depths between 0.1 and 1cm, with a mean of 0.4cm.

Coniform anomalies (Fig. 10A-D) were recognised in only four colonies, accounting for 5.4% of the colonies with skeletal anomalies (Table 1). These structures are circular and have diameters ranging between 3 and 4cm and heights up to 3cm, with a depressed central part measuring between 1 and 2.5cm (Fig. 10A-D). Their mean diameter and height are 3.5 and 2.6cm, respectively.

In the 68% of the corals, the margins of the skeletal anomalies are smooth (*e.g.* Figs. 5; 6A, C, E; 7A, E), in the 11.1% are uneven (*e.g.* Figs. 7C; 12A) and in the other 20.9% smooth and uneven (Table 1). The edges of the skeletal lesions observed in the corals are mainly distinct, noted in 94.4% of the corals analysed with damage (*e.g.* Figs. 6A, C, E; 7A, C, E; 8A, C, D; 10A-D; 11A). However, smaller portions, constituting 4.2% and 1.4% of the coral colonies with anomalies, respectively display skeletal lesions with both distinct and annular, or only annular edges (Fig. 9A).

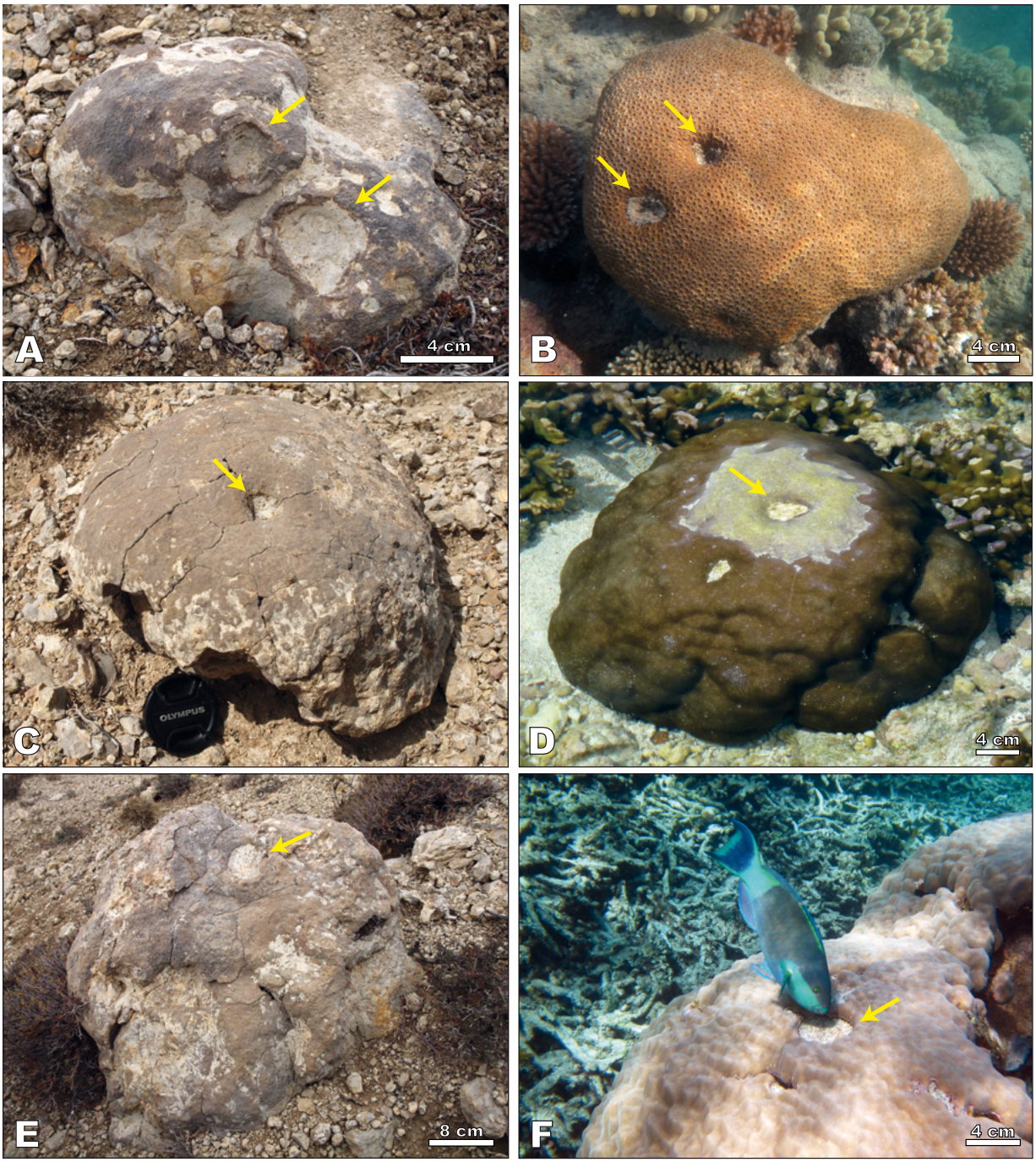

FIGURE 6. Depressed skeletal anomalies with circular shape. A) Coral colony from Villarroya de los Pinares exhibiting two depressed circular skeletal anomalies (yellow arrows), alongside a linear to irregular anomaly. The margins and edges of the damaged areas are respectively smooth and distinct. Note how the circular depressioms exhibit overgrown margins. The distribution of the anomalies is multifocal and their location on the colony is basal to apical. B) A living coral colony photographed in the Whitsunday Islands (Great Barrier Reef; eastern Australia) displaying two depressed circular lesions (yellow arrows) comparable to those shown in Figure 6A. C) Domal coral exhibiting a depressed circular anomaly with a smooth margin, a distinct edge, and a focal distribution (yellow arrow). The skeletal anomaly severity is mild and the damage location on colony is apical. The specimen was photographed in the Barranco de las Corralizas. Camera cap= 5.8cm. D) Colonial coral from the lagoon of Lady Elliot Reef (Great Barrier Reef; eastern Australia) with an apically located depressed circular skeletal anomaly (yellow arrow), morphologically resembling the anomaly on the coral shown in Figure 6C. Discoloration surrounding the circular depression indicates the presence of dead coral tissue, a result of subaerial exposure during low tide. E) Close-up view of a coral colony from Villarroya de los Pinares showing a depressed part of the skeleton with a circular shape (yellow arrow), a smooth margin and a distinct edge. Note the presence of several other irregular anomalies. The distribution of skeletal lesions on the colony is multifocal and the extent of the anomalies is severe. F) Detailed view of a circular denuded area, showcasing a loss of live coral cover in a colony from Coral Bay in Ningaloo Reef (western Australia), similar to the one photographed in Figure 6E. Note the presence of the sixband parrotfish *Scarus frenatus*, actively feeding on microscopic autotrophs (see *e.g.* Clements *et al.*, 2017) that has proliferated on the damaged tissue surface.

The distribution of skeletal anomalies on the colonies is primarily multifocal, observed in 65.2% of the colonies exhibiting damage structures (Table 1; Figs. 6A, E; 8A, C; 10A-B; 12A). Conversely, 34.8% of the corals with anomalies display only one single skeletal lesion, and thus a focal distribution (Figs. 6C; 7A; 10D; 11A). The location of skeletal anomalies on the colonies is mainly apical, accounting for 55.5% of the colonies with skeletal lesions (Table 1; Figs. 6C; 7A, C; 9C; 10D; 11A). Additionally, 30.6% of the corals with anomalies display skeletal lesions with medial and apical locations (Figs. 8A, E; 10A; 12A). Furthermore, 7% of the corals exhibit damage located medially, and the remaining 5.5% present anomalies with basal, medial and apical locations (Figs. 6A; 8C; 9E). Only one coral colony, representing 1.4% of the colonies with anomalies, was observed exhibiting skeletal lesions located basally and medially. Finally, the severity of the damage observed is mild (Figs. 6C; 7A), moderate (Figs. 7E; 8A, C), severe (Figs. 9C), and extreme (Fig. 9E), in the 37.5%, 37.5%, 23.6% and 1.4% of the colonies with skeletal anomalies, respectively (Table 1).

Post-mortem bioerosion, characterized by structures lacking significant relief, is widespread among the colonies surveyed. The perforations were originally depressed areas of the skeleton which were subsequently infilled by micrite and/or sparry calcite and are thus distinguished from the rest of the skeleton by lighter, usually whitish, coloration (Figs. 11A-B; 12C-D; 13-14). These no-relief structures mainly display circular shapes in equatorial sections (Figs. 11B; 12D) and are oblong in longitudinal sections (Fig. 11B, D). Their diameters range from 0.2 to 2.2cm, with a mean of 0.9cm. Frequently, these circular to oblong structures are found in walls and floors of depressed skeletal lesions and thus, postdate the formation of the anomaly (Fig. 14). Locally, they also exhibit *in situ* valves of lithophagid bivalves (Fig. 11D). Circular to oblong post-mortem bioerosion features produced by lithophagid bivalves were recognised in 50 out of the 102 colonies examined.

Further post-mortem no-relief bioerosion includes rare ramified (Fig. 12C-D) and linear (Fig. 13) structures. The ramified bioerosion features have lengths from 3 to 6.5cm, and widths from 0.1 to 0.2cm. The linear structures show lengths between 0.6 and 1.8cm, with a mean of 1.3cm, and widths between 0.1 and 0.2cm. Some of the no-relief linear structures recognised show curved, U-shaped forms (Fig. 13B-D). Ramified and linear post-mortem bioerosion was recognised in 2 and 13 out of the 102 scleractinians investigated, respectively.

DISCUSSION

Tissue loss due to environmental stress experienced by the coral polyps or physical damage in scleractinian corals modifies the growth of the corallites around the wound area (*e.g.* Work and Rameyer, 2005). These corallite anomalies represent a localised response of the living coral tissue to injury. Following injury, the coral tissue may regenerate to seal the damaged area (*e.g.* Work and Aeby, 2010), or the coral skeleton may remain exposed (Figs. 6B, D; 7B, F; 8D, F; 9D, F; 10E-F; 11C; 12B), potentially being covered by red algae, turf algae, microbes, or sediment (Fig. 7D) (*e.g.* Fisher *et al.*, 2007).

The depressed and coniform skeletal anomalies described in the Aptian corals strongly resemble gross lesions observable in living corals (Figs. 6-11A, C; 12A-B). To ensure the validity of this analogy, it is crucial to determine whether these fossil skeletal anomalies occurred prior to the death of the scleractinian colonies or not. The original aragonite of the coral skeletons was replaced by calcite during burial. Throughout this process, the corallite structures underwent recrystallization, hindering the observation of corallite anomalies around the margins of the damaged skeletal area. However, the fossil coniform structures identified (Fig. 10A-D) were the result of upward growth towards the centre of a damaged area and thus, indicate regenerative processes (*e.g.* Lirman, 2000). In recent corals, similar coniform structures (Fig. 10E-F) result from symbiotic relationships with other fauna such as pyrgomatid barnacles (*e.g.* Chan *et al.*, 2013; Yap *et al.*, 2023) or cryptochirid crabs (*e.g.* Wong *et al.*, 2023). In line with this, living colonies infested with symbiotic polychaetes also develop aberrant growth forms consisting of deformations of the coral skeleton around the worm tubes (*e.g.* Wielgus *et al.*, 2006). Thus, the coniform-shaped anomalies (Fig. 10A-D) observed in the Aptian scleractinians are indicative of regeneration, ergo, of an ante-mortem process.

The post-mortem bioerosion features currently showing no significant relief usually exhibit irregular ramified (Fig. 12C-D), linear (Fig. 13) and circular to oblong shapes (Figs. 11A-B, D; 12D). The origin of the irregular ramified structures lacking relief (Fig. 12C-D) is unknown. The linear structures are often U-shaped (Fig. 13). These convoluted forms are likely traces left by worms (*e.g.* Sammarco and Risk, 1990). On the other hand, the circular to oblong ichnofossils lacking significant relief (Figs. 10A-C; 11A-B; 12D) frequently contain lithophagid bivalves (Fig. 11D), and thus can be ascribed to the ichnogenus *Gastrochaenolites* (Kelly and Bromley, 1984). The lack of skeletal overgrowth around the *Gastrochaenolites* (Figs. 11A-B, D; 12D; 14A), ramified structures (Fig. 12C-D) and annelid traces (Fig. 13) observed indicates absence of tissue regeneration and thus, the infestation of the colonies by boring organisms, or other colonizers, likely occurred after their death.

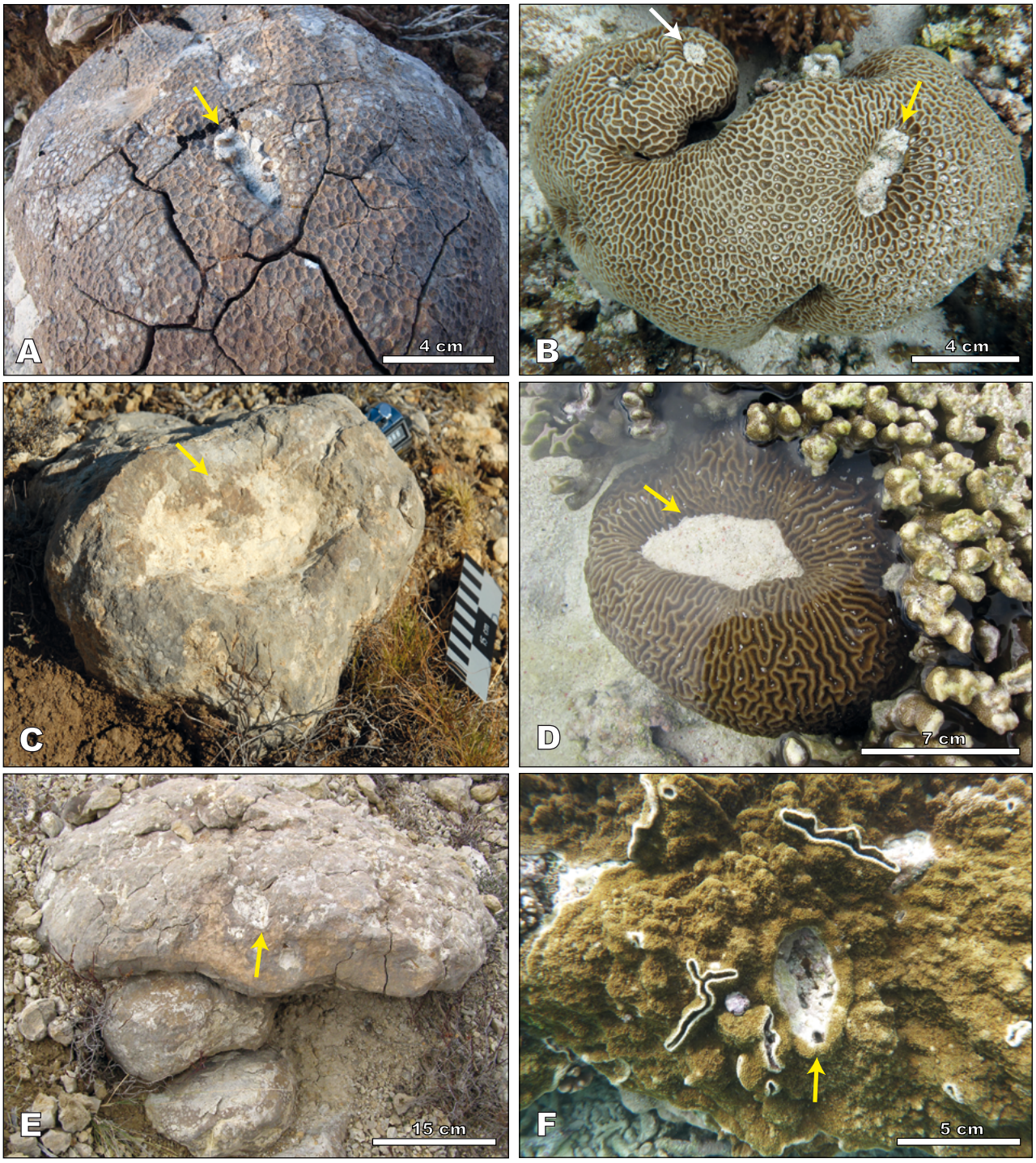

FIGURE 7. Depressed skeletal anomalies with oblong shape. A) Domal coral colony from the Barranco de las Corralizas exhibiting a depressed oblong lesion with a smooth margin, and distinct edge (yellow arrow). The distribution and location of the skeletal anomaly is focal and apical, respectively. The skeletal anomaly severity is mild. B) Living coral from Lady Elliot Reef lagoon (Great Barrier Reef; eastern Australia) with an apical oblong lesion (yellow arrow) similar to that shown in Figure 7A. White arrow points to a circular lesion comparable to those displayed in Figure 6A, C, E. C) Close-up view of a colony with an oblong skeletal anomaly with an uneven margin and a distinct edge (yellow arrow). The distribution of skeletal anomalies on the colony is focal, and their location is apical. The specimen was photographed in the Barranco de las Corralizas. Ruler= 15cm. D) Colonial coral from the lagoon of Lady Elliot Reef (Great Barrier Reef; eastern Australia) showing a depressed oblong lesion (yellow arrow) like the one in Figure 7C. Note that the denuded oblong lesion is partially filled with sediment. E) Coral skeleton from the Barranco de las Corralizas exhibiting diverse damage structures including an oblong skeletal anomaly with a smooth margin and a distinct edge (yellow arrow). The skeletal anomaly severity is moderate, the distribution of anomalies is multifocal, while their location is basal to apical. Note that the coral showing the oblong-shaped damage grew on top of other smaller colonies. F) Detailed view of a denuded oblong wound (yellow arrow) in a living colony from Coral Gardens in Lady Elliot Reef (Great Barrier Reef; eastern Australia). This oblong lesion is comparable to the damage structure shown in Figure 7E.

FIGURE 8. Depressed skeletal anomalies with pyriform and linear shapes. A) Domal coral colony from the Barranco de las Corralizas exhibiting anomalies with circular (white arrow) and pyriform (yellow arrow) shapes, with margins that range from uneven to smooth, and distinct edges. The anomalies are distributed multifocally and located medially to apically. The severity of the skeletal lesions is moderate. B) Recent dead coral from Lady Elliot Island (Great Barrier Reef; eastern Australia), exhibiting similar pyriform (yellow arrow) and circular (white arrow) lesions as shown in Figure 8A. C) Close-up view of a depressed linear skeletal anomaly with a smooth margin and a distinct edge (yellow arrow). Note the presence of a smaller scale irregular anomaly on the lower left side of the colony. The skeletal lesion distribution on the colony is multifocal, the location is basal to apical, and the severity is moderate. The specimen was photographed in Villarroya de los Pinares. D) Domal coral from the lagoon of the Whitsunday Islands (Great Barrier Reef; eastern Australia) showing a denuded linear lesion (yellow arrow) similar to the anomaly shown in Figure 8C. E) Close-up view of severe linear anomalies on a coral skeleton (yellow arrow) from the marls of the lower part of the Benassal Formation in Las Mingachas. The margins of the damaged areas are smooth, and the edges are distinct. The distribution of skeletal anomalies is multifocal, and their location on the colony is medial to apical. F) Detailed view of denuded linear skeletal anomalies (yellow arrow) in a coral from the Whitsunday Islands (Great Barrier Reef; eastern Australia) exhibiting similar lesion patterns as those photographed in Figure 8E.

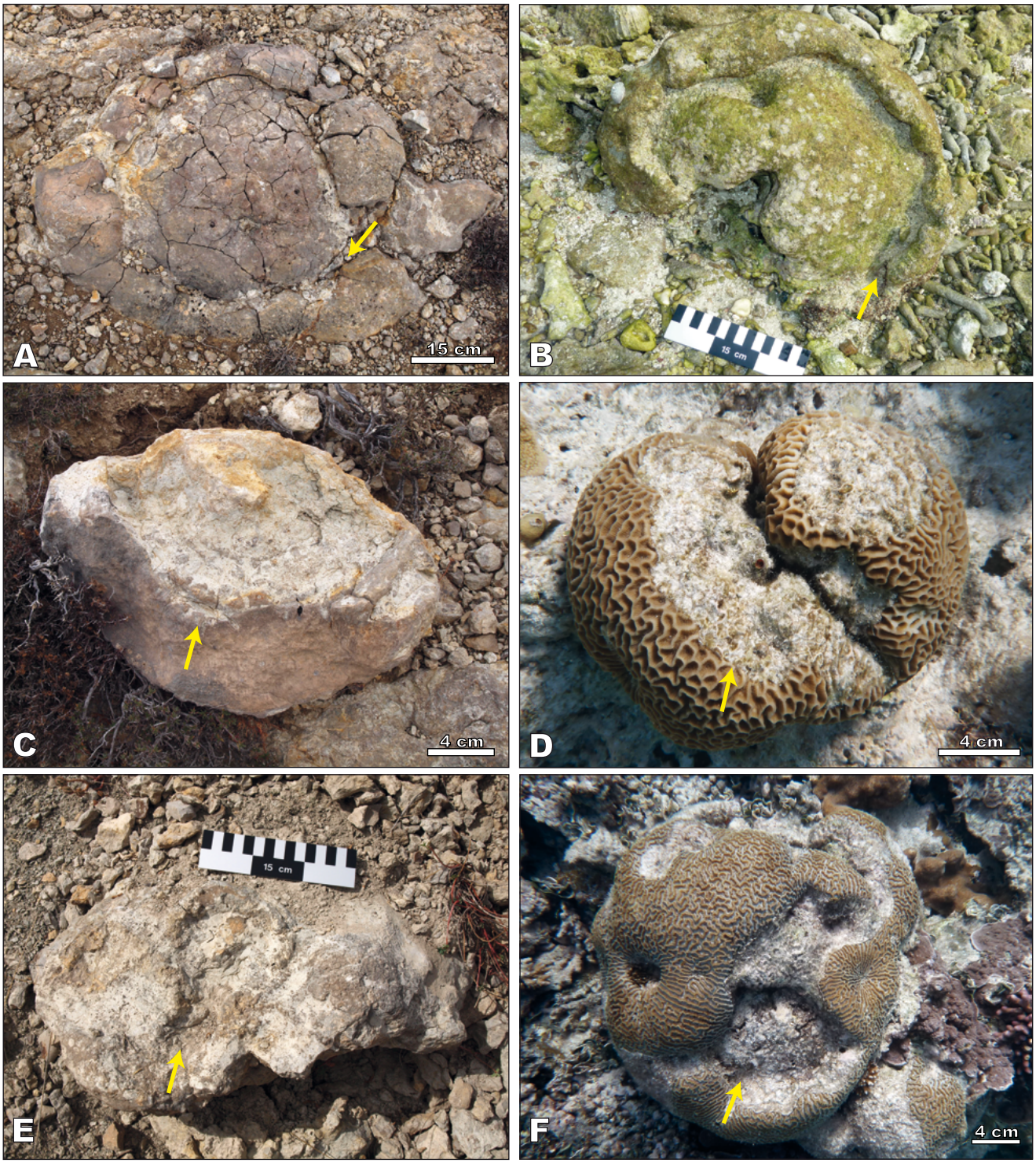

FIGURE 9. Depressed skeletal anomalies with linear and irregular shapes. A) A coral from Villarroya de los Pinares displaying a depressed linear damage with an uneven margin and an annular edge (yellow arrow). B) A dead coral overgrown by green algal filaments from Lady Elliot Reef (Great Barrier Reef; eastern Australia) showcasing a denuded linear lesion with an annular edge (yellow arrow), akin to the anomaly presented in Figure 9A. C) Coral showing a severe depressed irregular anomaly at the apical region of the colony (yellow arrow). The specimen was photographed in the Villarroya de los Pinares. D) Colonial coral from Wistari Reef (Great Barrier Reef; eastern Australia) showing a denuded irregular skeletal anomaly with an uneven margin and a distinct edge, located on the apical region (yellow arrow). This irregular skeletal damage to a living colony resembles the fossil example shown in Figure 9C. E) Coral colony from the Barranco de las Corralizas exhibiting an extreme depressed irregular skeletal anomaly with a basal to apical location (yellow arrow). F) Living colony from Blue Pools on Heron Reef (Great Barrier Reef; eastern Australia) exhibiting an extreme irregular denuded lesion similar to the one in Figure 9E.

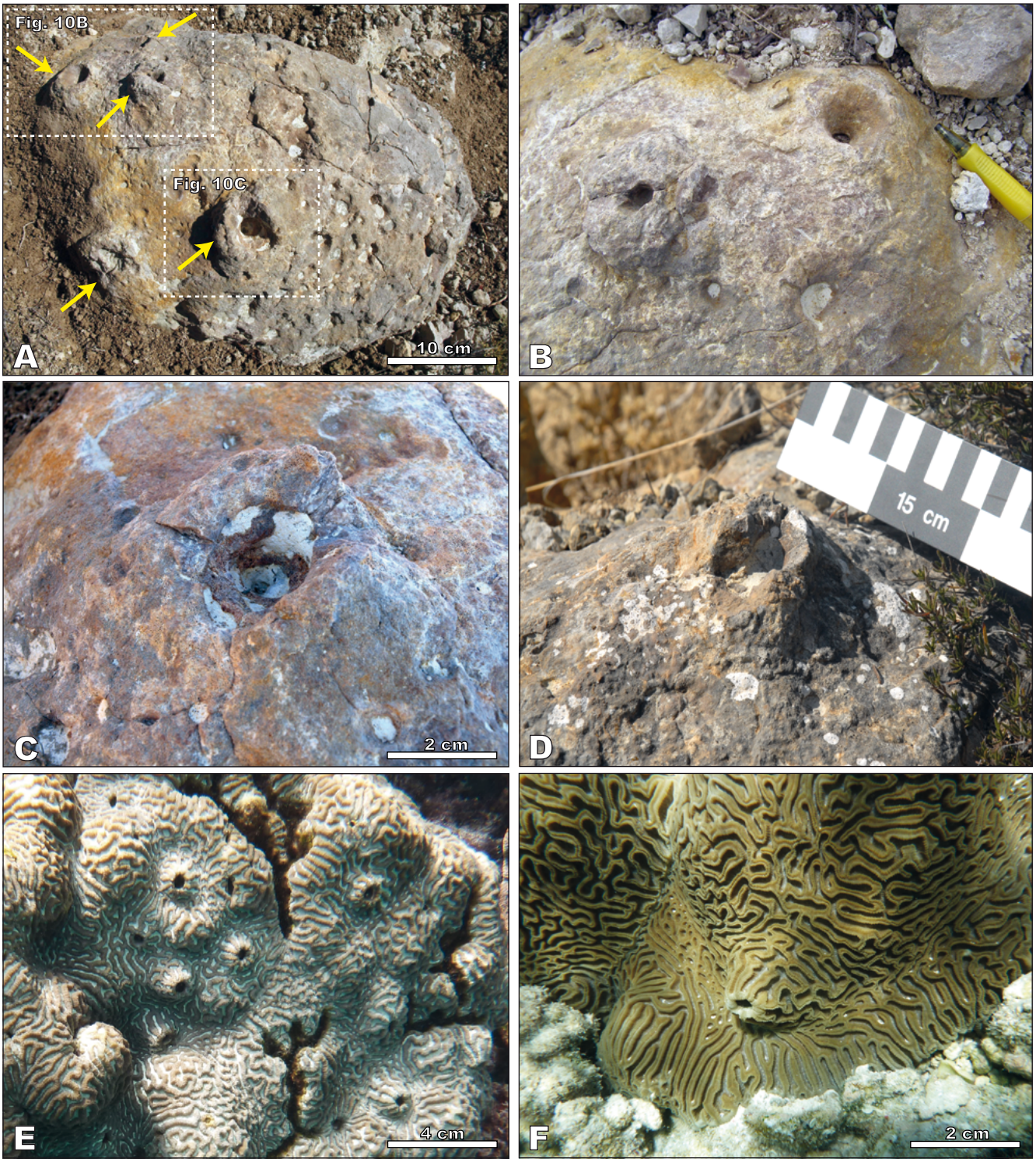

FIGURE 10. Coniform skeletal anomalies. A) Domal coral colony from the Barranco de las Corralizas exhibiting five coniform skeletal anomalies (yellow arrows) and abundant *Gastrochaenolites* borings. Skeletal anomalies are severe, and show circular shapes, smooth margins, distinct edges, a multifocal distribution, and a medial to apical location. B) Detail of Figure 10A showing three overgrowth structures around damaged areas. Visible part of pen= 5cm. C) Close-up view of one of the coniform skeletal anomaly present in the coral colony shown in Figure 10A. D) Detail of an aberrant overgrowth structure present on a coral from the Barranco de las Corralizas. The skeletal anomaly severity is mild, the relief is coniform, the shape is circular, the margin is uneven, the edge is distinct, the distribution is focal, and the location is apical. E-F) Coniform skeletal anomalies on *Platygyra* corals from Lady Elliot Island (eastern Australia). In modern corals, such overgrowth structures are the result of symbiotic association with pyrgomatid barnacles (*e.g.* Chan *et al.*, 2013) or cryptochirid crabs (*e.g.* Wong *et al.*, 2023).

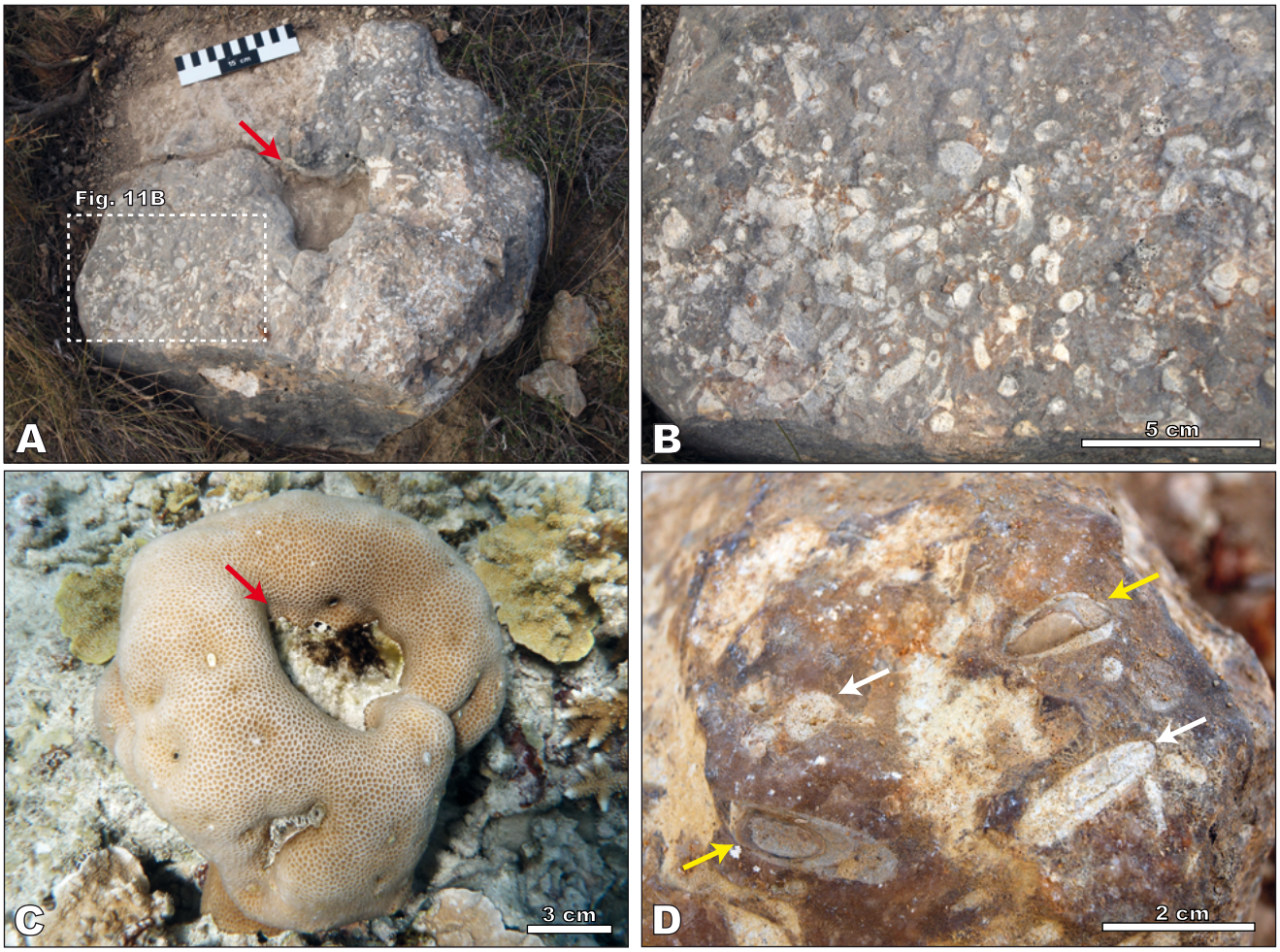

FIGURE 11. Depressed irregular skeletal anomalies and post-mortem bioerosion by lithophagid bivalves. A) Domal coral colony from the lowermost marls of the Benassal Formation in Las Mingachas exhibiting abundant post-mortem circular to oblong *Gastrochaenolites*. The red arrow points to a central apical depressed lesion with an irregular shape. B) Detail of Figure 11A showing abundant *Gastrochaenolites*. C) Living coral from Knuckle Reef (Great Barrier Reef; eastern Australia) showing an apical irregular denuded lesion (red arrow) similar to the skeletal anomaly shown in Figure 11A. Note the small white spots, that probably correspond to holes of symbiotic worms such as *Spirobranchus*. D) Close-up view of a coral from the Barranco de las Corralizas exhibiting equatorial to axial sections of post-mortem *Gastrochaenolites* borings (white arrows) and the valves of the lithophagid bivalve preserved *in situ* (yellow arrows).

In contrast, some of the depressed skeletal anomalies examined underwent regeneration, as inferred from the overgrowth features noticed around their margins (*e.g.* Figs. 6A; 8E). Furthermore, the walls and floors of several circular, oblong, pyriform and irregular anomalies, were bored by lithophagid bivalves (Fig. 14), indicating that their formation occurred prior to lithophagine settlement. While most of the current species of lithophagid bivalves penetrate corals after death (Kleemann, 1980), or show a preference for dead portions of living colonies (Wilson, 1979), only a few have the ability to bore into living tissue (Kleemann, 1980; Jones and Pemberton, 1988). Consequently, the depressed skeletal anomalies described in the fossil corals are interpreted to have been bored (Fig. 14) after tissue loss and probable further skeletal damage by bioeroding and grazing animals (*e.g.* see Fig. 6F). Therefore, the depressions documented would have been formed before the death of the colonies. Given that the ante-mortem skeletal anomalies observed likely originated from tissue loss during the specimens' lifetime, they conform to the criteria of a lesion as defined by Work and Aeby (2006).

In many cases, as the coral colony is growing, only the upper and outer part exposed to sunlight is covered by the living tissue, while the older, basal part of the colony is dead. Consequently, ante-mortem and post-mortem processes can occur at the same time in the same colony, albeit at different places.

Concerning the aetiologic diagnosis of the depressed skeletal anomalies studied (Figs. 6A, C, E; 7A, C, E;

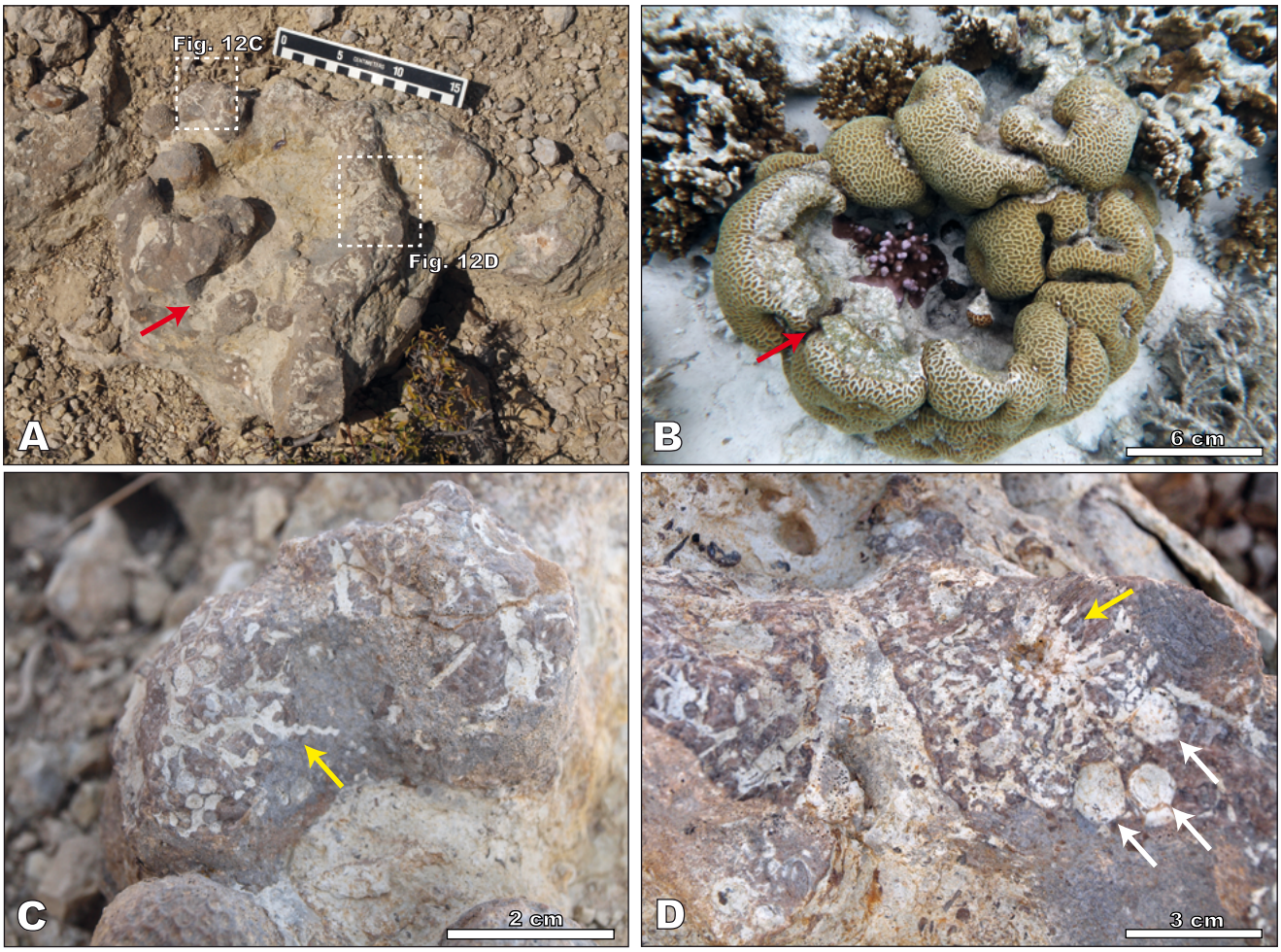

FIGURE 12. Depressed irregular skeletal anomalies and post-mortem ramified traces. A) Coral from the Barranco de las Corralizas exhibiting an extreme depression and highly irregular loss of the skeleton with uneven margins, distinct edges, a multifocal distribution, and a medial to apical location (red arrow). The non-depressed part of the colony displays smaller scale post-mortem ramified structures showing no relief. B) Modern colonial coral photographed in Shark Bay on Heron Reef (Great Barrier Reef; eastern Australia) showing a denuded and highly irregular apical lesion (red arrow) comparable to the anomaly shown in Figure 12A. C-D) Close-up views of the non-depressed part of the coral colony displayed in Figure 12A showing ramified post-mortem traces with no relief (yellow arrows). Circular features corresponding to *Gastrochaenolites* borings are marked with white arrows.

8A, C, E; 9A, C, E; 10A-D; 11A; 12A), the presence of *Gastrochaenolites* postdating damage (Fig. 14) rules out the possibility that these fossil anomalies were the result of post-mortem chemical dissolution during burial diagenesis or by recent rainwater, given the current subaerial exposure of the colonies (Figs. 2-3). The ante-mortem skeletal anomalies described are comparable to tissue lesions and skeletal denudation produced in modern corals either by predation (corallivorous fish, snails, worms, starfish) (*e.g.* Cole *et al.*, 2008; Dalton and Godwin, 2006; De'ath *et al.*, 2012; Robertson, 1970), bioerosion (grazing fish, algae, sea urchins, fungi, crustaceans, molluscs, worms) (*e.g.* Benzoni *et al.*, 2010; Chazottes *et al.*, 1995; Holmes *et al.*, 2000; Morais *et al.*, 2022a; Ong and Holland, 2010), sediment veneering (*e.g.* Erftemeijer *et al.*, 2012; Weber *et al.*, 2012), physical impact (storms) (*e.g.* Harmelin-Vivien, 1994), tidally-controlled subaerial conditions (see Fig. 6D), competition for primary space (algal and sponge overgrowth) (*e.g.* Coles and Bolick, 2007; Eckrich and Sabine Engel, 2013) and disease (*e.g.* Richardson, 1998; Sutherland *et al.*, 2004). For example, black band disease commonly creates circular denuded areas on coral heads (*e.g.* Kuta and Richardson, 2002), comparable to those seen in the Aptian corals. Furthermore, large vertebrate (*e.g.* turtles) activities such as landing, resting, leaving, scratching, and foraging on corals can also produce damage to scleractinian tissues and skeletons (Bennett *et al.*, 2000).

The possibility that the skeletal depressed anomalies reported could have formed ante-mortem by physical impact produced by storms and/or subaerial exposure at low tide, seems unlikely. The corals studied developed

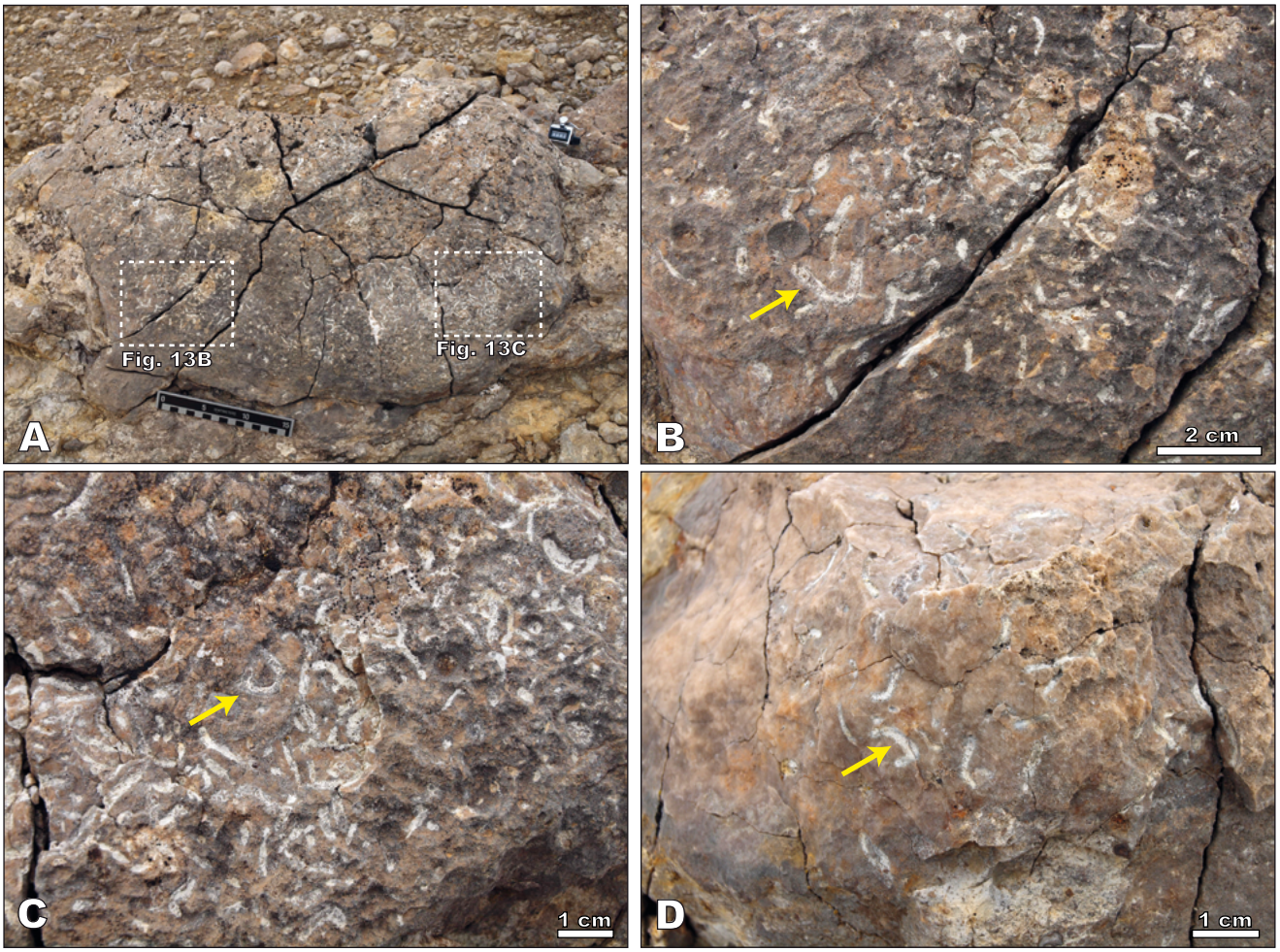

FIGURE 13. Post-mortem traces with linear shapes. A) Domal coral colony from Villarroya de los Pinares exhibiting abundant post-mortem no-relief traces with linear shapes. B-C) Close-up views of the post-mortem traces exhibited by the skeleton of the coral colony displayed in Figure 13A. Yellow arrows point to curved, U-shaped structures interpreted as manifestations of worm activity. D) Detail of linear to curve-shaped post-mortem traces present in a colony from Villarroya de los Pinares. Yellow arrow points to a U-shaped structure.

as isolated colonies (Figs. 2; 6A, C, E; 7A, C, E; 8A, C, E; 9A, C, E; 10A; 11A, D; 12A; 13A; 14A) giving rise to non-reefal level-bottom communities (Fig. 3) *sensu* Riding (2002), in marly slope environments, and thus in slightly deeper positions than their corresponding carbonate platform tops (Bover-Arnal *et al.*, 2012, 2015). No overturned or tilted colonies have been identified, which would indicate high-energy episodes due to storm or wave action (see also Bover-Arnal *et al.*, 2012). Along these lines, within the marls embedding the colonies, fragmented hard skeletal parts of organisms that could have acted as projectiles injuring coral tissues and/or eroding skeletons during storms were not recognised. Furthermore, many of the linear, pyriform, and massive irregular forms exhibited by the anomalies observed (*e.g.* Figs. 7B; 8C, E; 9A, C, E; 11A; 12A) do not match with those that would be expected from a projectile impact.

Exposure to sedimentation, resulting in tissue necroses due to burial of coral polyps, is not likely to have been the primary cause of coral damage in such calm distal environments with low sedimentation rates (see Bover-Arnal *et al.*, 2012, 2015). Competition for primary space and destructive activities by large vertebrates are not currently major factors causing damage to corals, and it is not expected that they were significant in the past. Consequently, the most plausible mechanisms that produced skeletal anomalies in the Aptian corals studied are predation, bioerosion, and disease.

The ante-mortem skeletal anomalies in the studied fossil corals do not allow for discrimination between lesions caused by disease, or by tissue loss and skeletal damage by predation and/or bioerosion. In fact, even in living corals, distinguishing between tissue loss or skeletal damage caused by disease and that produced by predation is

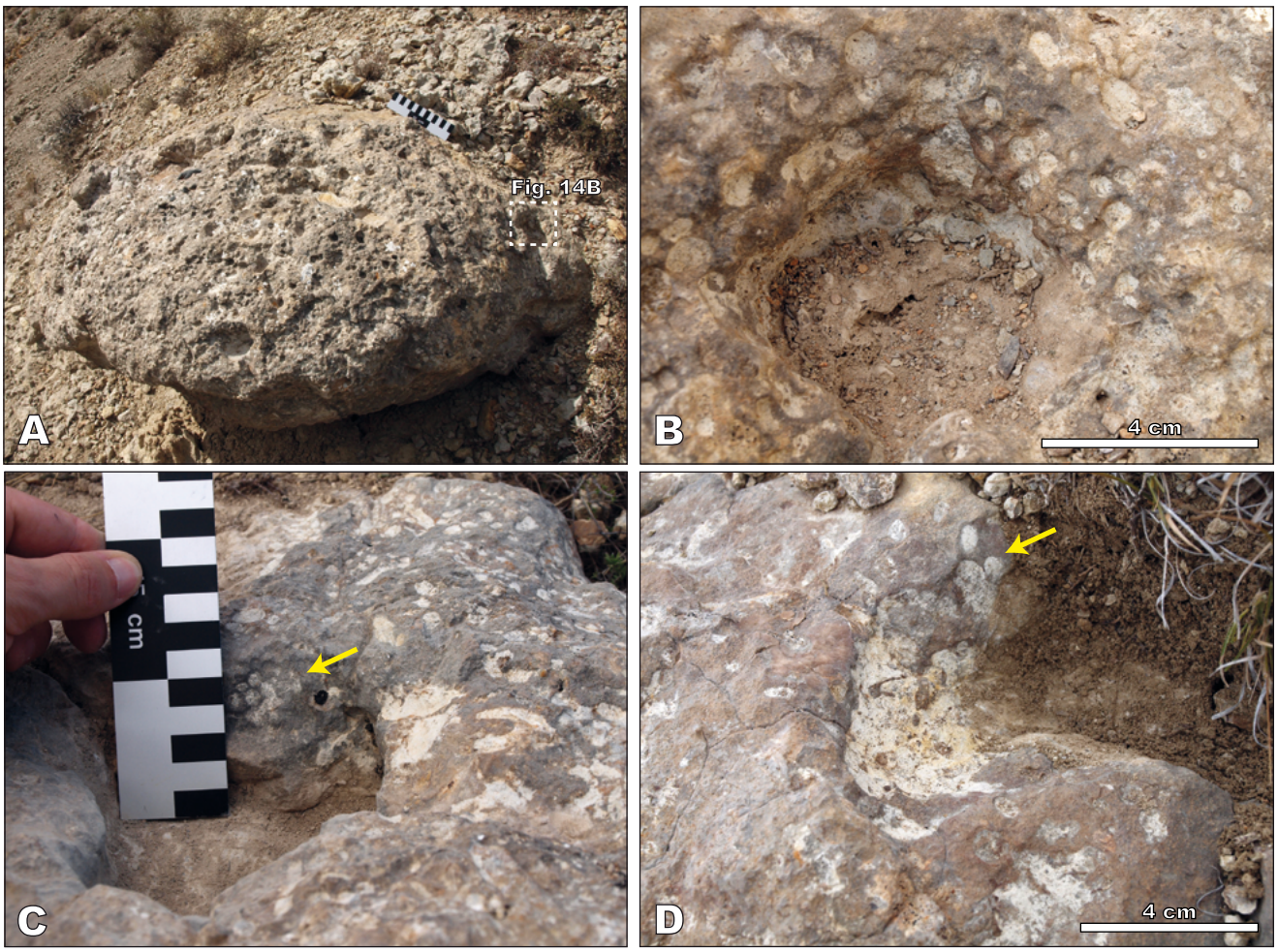

FIGURE 14. Depressed large skeletal anomalies overprinted by post-mortem *Gastrochaenolites* borings. A) Domal coral colony from the Barranco de las Corralizas exhibiting *Gastrochaenolites* and depressed skeletal anomalies with circular to oblong shapes, smooth margins, and distinct edges. The anomalies are multifocal in distribution and located medially to apically. Ruler= 15cm. B) Detail view of Figure 14A highlights abundant *Gastrochaenolites* borings postdating a previous circular depressed region of the skeleton. C) Close-up view of a depressed part of the coral skeleton shown in Figure 11A-B from the lower part of the Benassal Formation in Las Mingachas postdated by equatorial sections of *Gastrochaenolites* borings (yellow arrow). D) Colonial coral from Villarroya de los Pinares showing a depressed irregular skeletal anomaly with an uneven margin, a distinct edge, and an apical location. The walls of this depressed part of the skeleton exhibit post-mortem *Gastrochaenolites* (yellow arrow).

often impossible (Sutherland *et al.*, 2004; Work and Aeby, 2006). This difficulty arises because predation scars often resemble signs of disease. In this regard, Work and Aeby (2006) state that, in the field, the aetiological diagnosis between disease and predation is often only possible if the predator is caught in action. Sutherland *et al.* (2004) point out that the most effective method to differentiate between disease and predation is to observe the progression of the coral lesion in the absence of predators under laboratory conditions or by foraging predators from the natural environment. Therefore, if distinguishing between disease and predation already poses challenges in the present and microscopic biological laboratory investigations are often necessary (Work and Aeby, 2006), determining the origin of coral skeletal anomalies in the fossil record becomes even more challenging.

CONCLUSIONS

The skeletal anomalies observed, including depressions and coniforms, provide rare evidence of ante-mortem damage in Aptian coral skeletons. The frequent occurrence of overgrown margins and *Gastrochaenolites* borings on depressed skeletal regions, along with coniform anomalies indicative of skeletal overgrowth due to damage, strongly support their ante-mortem origin. The resemblance of these fossil skeletal anomalies to lesions observed in modern corals is particularly noteworthy, reinforcing the idea that similar biological processes were at play during the Cretaceous. The observed ante-mortem skeletal anomalies are likely attributable to predation, bioerosion, and/or disease, with disease being a potentially significant but underappreciated factor in fossil coral records. This study

underscores the fossilization potential of coral anomalies resulting from tissue lesions and skeletal damage, a factor that may have been significantly underestimated in previous research on fossil coral communities. Finally, these findings contribute to a more accurate understanding of the biological and ecological dynamics of Cretaceous coral ecosystems.

ACKNOWLEDGMENTS

We would like to thank Marco Brandano, an anonymous reviewer, and the guest editor Josep Anton Moreno-Bedmar for their valuable suggestions, which improved the final version of the manuscript. This contribution benefited from fruitful discussions with Greta Aeby and Thierry Work. We are grateful to the editorial staff: Miguel Garcés, Eulàlia Gili, and Laura Rincón, for their assistance in refining the article, enhancing the accuracy of the terminology used, and improving the overall fluency of the English. Financial support provided by the Grup de Recerca Reconegut per la Generalitat de Catalunya 2021 SGR-Cat 00349 "Geologia Sedimentària", the Swiss National Science Foundation (grant 20-121545) and the I+D+i research project IBERINSULA (PID2020-113912GB-I00), funded by MCIN/AEI/10.13039/501100011033 and the European Regional Development Fund (ERDF), is acknowledged.

REFERENCES

Aeby, G.S., Ushijima, B., Campbell, J.E., Jones, S., Williams, G.J., Meyer, J.L., Häse, C., Paul, V.J., 2019. Pathogenesis of a tissue loss disease affecting multiple species of corals along the Florida reef tract. Frontiers in Marine Science, 6, 678, 1-18.

Álvarez-Pérez, G., Busquets, P., 2012. Formas anómalas en los corales eocenos de la Cuenca de Igualada (Noreste de España). [Anomalous forms of the Eocene corals in the Igualada Basin (North-East Spain)]. Revista Española de Paleontología, 27, 15-28.

Bennett, P., Keuper-Bennett, U., Balazs, G.H., 2000. Changing the landscape: evidence for detrimental impacts to coral reefs by Hawaiian marine turtles. Proceedings of the twentieth annual symposium on sea turtle biology and conservation. 29 February-4 March 2000, Orlando (Florida, U.S.A.), NOAA technical memorandum NMFS-SEFSC-477, 287-288.

Benzoni, F., Galli, P., Pichon, M., 2009. Pink spots on *Porites*: not always a coral disease. Coral Reefs, 29, 153.

Bover-Arnal, T., Salas, R., Moreno-Bedmar, J.A., Bitzer, K., 2009. Sequence stratigraphy and architecture of a late Early-Middle Aptian carbonate platform succession from the western Maestrat Basin (Iberian Chain, Spain). Sedimentary Geology, 219, 280-301.

Bover-Arnal, T., Moreno-Bedmar, J.A., Salas, R., Skelton, P.W., Bitzer, K., Gili, E., 2010. Sedimentary evolution of an Aptian syn-rift carbonate system (Maestrat Basin, E Spain): effects of accommodation and environmental change. Geologica Acta, 8(3), 249-280.

Bover-Arnal, T., Salas, R., Martín-Closas, C., Schlagintweit, F., Moreno-Bedmar, J.A., 2011. Expression of an oceanic anoxic event in a neritic setting: Lower Aptian coral rubble deposits from the western Maestrat Basin (Iberian Chain, Spain). Palaios, 26, 18-32.

Bover-Arnal, T., Löser, H., Moreno-Bedmar, J.A., Salas, R., Strasser, A., 2012. Corals on the slope (Aptian, Maestrat Basin, Spain). Cretaceous Research, 37, 43-64.

Bover-Arnal, T., Salas, R., Guimerà, J., Moreno-Bedmar, J.A., 2014. Deep incision in an Aptian carbonate succession indicates major sea-level fall in the Cretaceous. Sedimentology, 61, 1558-1593.

Bover-Arnal, T., Pascual-Cebrian, E., Skelton, P.W., Gili, E., Salas, R., 2015. Patterns in the distribution of Aptian rudists and corals within a sequence-stratigraphic framework (Maestrat Basin, E Spain). Sedimentary Geology, 321, 86-104.

Bover-Arnal, T., Moreno-Bedmar, J.A., Frijia, G., Pascual-Cebrian, E., Salas, R., 2016. Chronostratigraphy of the Barremian-Early Albian of the Maestrat Basin (E Iberian Peninsula): integrating strontium-isotope stratigraphy and ammonoid biostratigraphy. Newsletters on Stratigraphy, 49, 41-68.

Canérot, J., Crespo, A., Navarro, D., 1979. Montalbán, hoja nº 518. Mapa Geológico de España 1:50.000. 2ª Serie. 1ª Edición. Madrid, Servicio de Publicaciones, Ministerio de Industria y Energía, 31pp.

Canérot, J., Cugny, P., Pardo, G., Salas, R., Villena, J., 1982. Ibérica Central-Maestrazgo. In: García, A. (ed.). El Cretácico de España. Madrid, Universidad Complutense de Madrid, 273-344.

Chan, B.K.K., Chen, Y.-Y., Lin, H.-C., 2013. Biodiversity and host specificity of coral barnacles of *Galkinia* (Cirripedia: Pyrgomatidae) in Taiwan, with descriptions of six new species. Journal of Crustacean Biology, 33, 392-431.

Chazottes, V., Le Campion-Alsumard, T., Peyrot-Clausade, M., 1995. Bioerosion rates on coral reefs: interactions between macroborers, microborers and grazers (Moorea, French Polynesia). Palaeogeography, Palaeoclimatology, Palaeoecology, 113, 189-198.

Clements, K.D., German, D.P., Piché, J., Tribollet, A., Choat, J.H., 2017. Integrating ecological roles and trophic diversification on coral reefs: multiple lines of evidence identify parrotfishes as microphages. Biological Journal of the Linnean Society, 120, 729-751.

Cole, A., Pratchett, M., Jones, G., 2008. Diversity and functional importance of coral-feeding fishes on tropical coral reefs. Fish Fisheries, 9, 286-307.

Coles, S., Bolick, H., 2007. Invasive introduced sponge *Mycale grandis* overgrows reef corals in Kane'ohe Bay, O'ahu, Hawai'i. Coral Reefs, 26, 911.

Cors, J., Heimhofer, U., Adatte, T., Hochuli, P.A., Huck, S., Bover-Arnal, T., 2015. Spore-pollen assemblages show

delayed terrestrial cooling in the aftermath of OAE 1a. Geological Magazine, 152, 632-647.

Dalton, S.J., Godwin, S., 2006. Progressive coral tissue mortality following predation by a corallivorous nudibranch (*Phestilla* sp.). Coral Reefs, 25, 529.

De'ath, G., Fabricius, K.E., Sweatman, H., Puotinen, M., 2012. The 27-year decline of coral cover on the Great Barrier Reef and its causes. Proceedings of the National Academy of Sciences, 109, 17995-17999.

Eckrich, C.E., Sabine Engel, M., 2013. Coral overgrowth by an encrusting red alga (*Ramicrusta* sp.): a threat to Caribbean reefs? Coral Reefs, 32, 81-84.

Elias, R.J., 1984. Paleobiologic significance of fossulae in North American Late Ordovician solitary rugose corals. Paleobiology, 10, 102-114.

Elias, R.J., 1986. Symbiotic relationships between worms and solitary rugose corals in the Late Ordovician. Paleobiology, 12, 32-45.

Erftemeijer, P.L.A., Riegl, B., Hoeksema, B.W., Todd, P.A., 2012. Environmental impacts of dredging and other sediment disturbances on corals: A review. Marine Pollution Bulletin, 64, 1737-1765.

Falces, S., 1997. Borings, embeddings and pathologies against microstructure. New evidences on the nature of the microstructural elements in rugose corals. Boletín de la Real Sociedad Española de Historia Natural (sec. Geológica), 92, 99-116.

Fisher, E.M., Fauth, J.E., Hallock, P., Woodley, C.M., 2007. Lesion regeneration rates in reef-building corals *Montastraea* spp. as indicators of colony condition. Marine Ecology Progress Series, 339, 61-71.

Garcia, R., Moreno-Bedmar, J.A., Bover-Arnal, T., Company, M., Salas, R., Latil, J.L., Martín-Martín, J.D., Gomez-Rivas, E., Bulot, L.G., Delanoy, G., Martínez, R., Grauges, A., 2014. Lower Cretaceous (Hauterivian–Albian) ammonite biostratigraphy in the Maestrat Basin (E Spain). Journal of Iberian Geology, 40, 99-112.

Gautier, F., 1980. Villarluengo, hoja nº 543. Mapa Geológico de España 1:50.000. 2ª Serie. 1ª Edición. Madrid, Servicio de Publicaciones, Ministerio de Industria y Energía, 45pp.

Gili, E., Skelton, P.W., Bover-Arnal, T., Salas, R., Obrador, A., Fenerci-Masse, M., 2016. Depositional biofacies model for post-OAE1a Aptian carbonate platforms of the western Maestrat Basin (Iberian Chain, Spain). Palaeogeography, Palaeoclimatology, Palaeoecology, 453, 101-114.

Guimerà, J., 1994. Cenozoic evolution of eastern Iberia: Structural data and dynamic model. Acta Geologica Hispanica, 29, 57-66.

Guimerà, J., 2018. Structure of an intraplate fold-and-thrust belt: The Iberian Chain. A synthesis. Geologica Acta, 16(4), 427-438.

Harmelin-Vivien, M.L., 1994. The effects of storms and cyclones on coral reefs: a review. Journal of Coastal Research, 12, 211-231.

Hoegh-Guldberg, O., Poloczanska, E.S., Skirving, W., Dove, S., 2017. Coral Reef Ecosystems under Climate Change and Ocean Acidification. Frontiers in Marine Science, 4, 158, 1-20.

Holmes, K.E., Edinger, E.N., Hariyadi, Limmon, G.V., Risk, M.J., 2000. Bioerosion of live massive corals and branching coral rubble on Indonesian coral reefs. Marine Pollution Bulletin, 40, 606-617.

Insalaco, E., 1998. The descriptive nomenclature and classification of growth fabrics in fossil scleractinian reefs. Sedimentary Geology, 118, 159-186.

Jones, B., Pemberton, S.G., 1988. Lithophaga borings and their influence on the diagenesis of corals in the Pleistocene Ironshore Formation of Grand Cayman Island, British West Indies. Palaios, 3, 3-21.

Kelly, S.R.A., Bromley, R.G., 1984. Ichnological nomenclature of clavate borings. Palaeontology, 27, 793-807.

Kleemann, K.H., 1980. Boring bivalves and their host corals from the Great Barrier Reef. Journal of Molluscan Studies, 46, 13-54.

Klompmaker, A.A., Portell, R.W., van der Meij, S.E.T., 2016. Trace fossil evidence of coral-inhabiting crabs (Cryptochiridae) and its implications for growth and paleobiogeography. Scientific Reports, 6, 23443, 1-11.

Knutson, T.R., McBride, J.L., Chan, J., Emanuel, K., Holland, G., Landsea, C., Held, I., Kossin, J.P., Srivastava, A.K., Sugi, M., 2010. Tropical cyclones and climate change. Nature Geoscience, 3, 157-163.

Kołodziej, B., Golubic, S., Bucur, I.I., Radtke, G., Tribollet, A., 2012. Early Cretaceous record of microboring organisms in skeletons of growing corals. Lethaia, 45, 34-45.

Kołodziej, B., Idakieva, V., Ivanov, M., Salamon, K., 2016. New record of endolithic algae syn vivo associated with an Early Cretaceous coral. Carnets de Géologie, 16, 633-640.

Kuta, K., Richardson, L., 2002. Ecological aspects of black band disease of corals: relationships between disease incidence and environmental factors. Coral Reefs, 21, 393-398.

Liesa, C.L., Soria, A.R., Meléndez, N., Meléndez, A., 2006. Extensional fault control on the sedimentation patterns in a continental rift basin: El Castellar Formation, Galve sub-basin, Spain. London, Journal of the Geological Society, 163, 487-498.

Lirman, D., 2000. Lesion regeneration in the branching coral *Acropora palmata*: effects of colonization, colony size, lesion size, and lesion shape. Marine Ecology Progress Series, 197, 209-215.

Martín-Chivelet, J., López-Gómez, J., Aguado, R., Arias, C., Arribas, J., Arribas, M.E., Aurell, M., Bádenas, B., Benito, M.I., Bover-Arnal, T., Casas-Sainz, A., Castro, J.M., Coruña, F., de Gea, G.A., Fornós, J.J., Fregenal-Martínez, M., García-Senz, J., Garófano, D., Gelabert, B., Giménez, J., González-Acebrón, J., Guimerà, J., Liesa, C.L., Mas, R., Meléndez, N., Molina, J.M., Muñoz, J.A., Navarrete, R., Nebot, M., Nieto, L.M., Omodeo-Salé, S., Pedrera, A., Peropadre, C., Quijada, I.E., Quijano, M.L., Reolid, M., Robador, A., Rodríguez-López, J.P., Rodríguez-Perea, A., Rosales, I.,

Ruiz-Ortiz, P.A., Sàbat, F., Salas, R., Soria, A.R., Suarez-Gonzalez, P., Vilas, L., 2019. The Late Jurassic–Early Cretaceous Rifting. In: Quesada, C., Oliveira, J.T. (eds.). The Geology of Iberia: A Geodynamic Approach. Volume 3: The Alpine Cycle. Heidelberg, Springer, 60-63. DOI: https://doi.org/10.1007/978-3-030-11295-0

Maynard, J., van Hooidonk, R., Eakin, C.M., Puotinen, M., Garren, M., Williams, G., Heron, S.F., Lamb, J., Weil, E., Willis, B., Harvell, C.D., 2015. Projections of climate conditions that increase coral disease susceptibility and pathogen abundance and virulence. Nature Climate Change, 5, 688-694.

Medellín-Maldonado, F., Cruz-Ortega, I., Pérez-Cervantes, E., Norzogaray-López, O., Carricart-Ganivet, J.P., López-Pérez, A., Alvarez-Filip, L., 2023. Newly deceased Caribbean reef-building corals experience rapid carbonate loss and colonization by endolithic organisms. Communications Biology, 6, 934, 1-11.

Morais, J., Morais, R., Tebbett, S.B., Bellwood, D.R., 2022a. On the fate of dead coral colonies. Functional Ecology, 36, 3148-3160.

Morais, J., Cardoso, A.P.L.R., Santos, B.A., 2022b. A global synthesis of the current knowledge on the taxonomic and geographic distribution of major coral diseases. Environmental Advances, 8, 100231.

Moreno-Bedmar, J.A., Company, M., Bover-Arnal, T., Salas, R., Maurrasse, F.J., Delanoy, G., Grauges, A., Martínez, R., 2010. Lower Aptian ammonite biostratigraphy in the Maestrat Basin (Eastern Iberian Chain, Eastern Spain). A Tethyan transgressive record enhanced by synrift subsidence. Geologica Acta, 8(3), 281-299.

Moreno-Bedmar, J.A., Bover-Arnal, T., Barragán, R., Salas, R., 2012. Uppermost Lower Aptian transgressive records in Mexico and Spain: chronostratigraphic implications for the Tethyan sequences. Terra Nova, 24, 333-338.

Oliver, W.A., 1983. Symbioses of Devonian rugose corals. Memoir of the Association of Australasian Palaeontologists, 1, 261-274.

Ong, L., Holland, K.N., 2010. Bioerosion of coral reefs by two Hawaiian parrotfishes: species, size differences and fishery implications. Marine Biology, 157, 1313-1323.

Richardson, L.L., 1998. Coral diseases: what is really known. Tree, 13, 438-443.

Riding, R., 2002. Structure and composition of organic reefs and carbonate mud mounds: concepts and categories. Earth-Science Reviews, 58, 163-231.

Roberts, C.M., 1995. Effects of Fishing on the Ecosystem Structure of Coral Reefs. Conservation Biology, 9, 988-995.

Robertson, R., 1970. Review of the predators and parasites of stony corals, with special reference to symbiotic prosobranch gastropods. Pacific Science, 24, 43-54.

Rotjan, R.D., Lewis, S.M., 2008. Impact of coral predators on tropical reefs. Marine Ecology Progress Series, 367, 73-91.

Salamon, K., Kołodziej, B., Löser, H., 2021. Diverse nature of ubiquitous microborings in Cenomanian corals (Saxonian Cretaceous Basin, Germany). Cretaceous Research, 126, 104888, 1-12.

Salamon, K., Kołodziej, B., Radtke, G., Schnick, H.H., Golubic, S., 2022. Microborings in Jurassic scleractinians: a glimpse into the ancient coral skeleton microbiome. Coral Reefs, 41, 863-867.

Salas, R., 1987. El Malm i el Cretaci inferior entre el Massís de Garraf i la Serra d'Espadà. Anàlisi de Conca. PhD Thesis. Barcelona, Universitat de Barcelona, 541pp. Website: http://hdl.handle.net/10803/669675

Salas, R., Casas, A., 1993. Mesozoic extensional tectonics, stratigraphy, and crustal evolution during the Alpine cycle of the eastern Iberian basin. Tectonophysics, 228, 33-55.

Salas, R., Guimerà, J., Mas, R., Martín-Closas, C., Meléndez, A., Alonso, A., 2001. Evolution of the Mesozoic Central Iberian Rift System and its Cainozoic inversion (Iberian Chain). In: Ziegler, P.A., Cavazza, W., Roberston, A.H.F., Crasquin-Soleau, S. (eds.). Peri-Tethys Memoir 6: Peri-Tethyan Rift/Wrench Basins and Passive Margins, 186. Paris, Mémoires du Muséum National d'Histoire Naturelle, 145-186.

Salas, R., García-Senz, J., Guimerà, J., Bover-Arnal, T., 2010. Opening of the Atlantic and development of the Iberian intraplate rift basins during the late Jurassic-early Cretaceous. In: Pena Dos Reis, R., Pimentel, N. (eds.). Rediscovering the Atlantic: New Ideas for An Old Sea. Lisbon 2010, II Central & north Atlantic Conjugate Margins Conference, Extended Abstracts, 3, 245-248. ISBN: 978-989-96923-1-2

Sammarco, P.W., Risk, M.J., 1990. Large-scale patterns in internal bioerosion of *Porites*: cross continental shelf trends on the Great Barrier Reef. Marine Ecology Progress Series, 59, 145-156.

Sanders, D., Baron-Szabo, R.C., 2005. Scleractinian assemblages under sediment input: their characteristics and relation to the nutrient input concept. Palaeogeography, Palaeoclimatology, Palaeoecology, 216, 139-181.

Santos, A., Mayoral, E., Gudveig Baarli, B., Da Silva, C.M., Cachão, M., Johnson, M.E., 2012. Symbiotic association of a Pyrgomatid barnacle with a coral from a volcanic Middle Miocene shoreline (Porto Santo, Madeira Archipielago, Portugal). Palaeontology, 55, 173-182.

Scoffin, T.P., Bradshaw, C., 2000. The taphonomic significance of endoliths in dead-versus live-coral skeletons. Palaios, 15, 248-254.

Simón, J.L., 2004. Superposed buckle folding in the eastern Iberian Chain, Spain. Journal of Structural Geology, 26, 1447-1464.

Sutherland, K.P., Porter, J.W., Torres, C., 2004. Disease and immunity in Caribbean and Indo-Pacific zooxanthellate corals. Marine Ecology Progress Series, 266, 273-302.

Tapanila, L., 2005. Palaeoecology and diversity of endosymbionts in Palaeozoic marine invertebrates: Trace fossil evidence. Lethaia, 38, 89-99.

Tapanila, L., 2006. Macroborings and bioclaustrations in a Late Devonian reef above the Alamo Impact Breccia, Nevada, USA. Ichnos, 13, 129-134.

Tapanila, L., Copper, P., 2002. Endolithic trace fossils in Ordovician-Silurian corals and stromatoporoids, Anticosti

Island, eastern Canada. Acta Geologica Hispanica, 37(1), 15-20.

Tapanila, L., Holmer, L.E., 2006. Endosymbiosis in Ordovician–Silurian corals and stromatoporoids: a new lingulid and its trace from eastern Canada. Journal of Paleontology, 80, 750-759.

Tapanila, L., Ekdale, A.A., 2007. Early History of Symbiosis in Living Substrates: Trace-Fossil Evidence from the Marine Record. In: Miller, W. (ed.). Trace Fossils. Concepts, Problems, Prospects. Amsterdam, Elsevier, 345-355. DOI: https://doi.org/10.1016/B978-044452949-7/50145-5

Vennin, E., Aurell, M., 2001. Stratigraphie sequentielle de l'Aptien du sous-basin de Galvé (Province de Teruel, NE de l'Espagne). Bulletin de la Société Géologique de France, 172, 397-410.

Vogel, K., 1993. Bioeroders in fossil reefs. Facies, 28, 109-113.

Webb, G.E., Yancey, T.E., 2010. Skeletal repair of extreme damage in rugose corals, Pella Formation (Mississippian, Iowa, USA). Palaeoworld, 19, 325-332.

Weber, M., de Beer, D., Lott, C., Polerecky, L., Kohls, K., Abed, R.M.M., Ferdelman, T.G., Fabricius, K.E., 2012. Mechanisms of damage to corals exposed to sedimentation. Proceedings of the National Academy of Science, 109, E1558-E1567.

Wielgus, J., Glassom, D., Chadwick, N.E., 2006. Patterns of polychaete worm infestation of stony corals in the northern Red Sea and relationships to water chemistry. Bulletin of Marine Science, 78, 377-388.

Wilson, B.R., 1979. A revision of Queensland Lithophagine mussels (Bivalvia, Mytilidae, Lithophaginae). Records of the Australian Museum, 32, 435-489.

Wong, K.J.H., Tsao, Y.-F., Qiu, J.-W., Chan, B.K.K., 2023. Diversity of coral-associated pit crabs (Crustacea: Decapoda: Cryptochiridae) from Hong Kong, with description of two new species of *Lithoscaptus* A. Milne-Edwards, 1862. Frontiers in Marine Science, 9, 1003321, 1-34.

Work, T.M., Rameyer, R.A., 2005. Characterizing lesions in corals from American Samoa. Coral Reefs, 24, 384-390.

Work, T.M., Aeby, G.S., 2006. Systematically describing gross lesions in corals. Diseases of Aquatic Organisms, 70, 155-160.

Work, T.M., Aeby, G.S., Coles, S.L., 2008. Distribution and morphology of growth anomalies in *Acropora* from the Indo-Pacific. Diseases of Aquatic Organisms, 78, 255-264.

Work, T.M., Aeby, G.S., 2010. Wound repair in *Montipora capitata*. Journal of Invertebrate Pathology, 105, 116-119.

Yap, F.-C., Chen, H.-N, Chan, B.K.K., 2023. Host specificity and adaptive evolution in settlement behaviour of coral-associated barnacle larvae (Cirripedia: Pyrgomatidae). Scientific Reports, 13, 9668.

Zande van der, R.M., Achlatis, M., Bender-Champ, D., Kubicek, A., Dove, S., Hoegh-Guldberg, O., 2020. Paradise lost: End-of-century warming and acidification under business-as-usual emissions have severe consequences for symbiotic corals. Global Change Biology, 26, 2203-2219.

Manuscript received April 2024;
revision accepted September 2024;
published Online November 2024.